



# A Data-Driven Approach to Structural Health Monitoring of Bridge Structures Based on the Discrete Model and FFT-Deep Learning

Thanh Q. Nguyen<sup>1,2</sup>

Received: 7 February 2021 / Revised: 25 May 2021 / Accepted: 18 June 2021 / Published online: 26 June 2021  
© Krishtel eMaging Solutions Private Limited 2021

## Abstract

In this paper, we investigate changes in the mechanical properties of complex structures using a combination of the discrete model, Fast Fourier Transform (FFT) analysis and deep learning. The first idea from this research utilizes the discrete model from a perspective that is different from the finite element method (FEM) of previous works. As the method in this paper only models the mechanical properties of structures with finite degrees of freedom instead of dividing them into smaller elements, it reduces error in evaluation and produces more realistic results compared to the FEM model. Another advantage is how it allows the research to survey both parameters that affect the mechanical properties of structures—the overall stiffness ( $K$ ) and the damping coefficient ( $c$ )—during vibration, while previous researches focus only on one of these two parameters. The second idea is to use FFT analysis to increase the sensitivity of the signal received during vibration. FFT analysis simplifies calculations, thereby reducing the effect of noise or errors. The sensitivity achieved in FFT analysis increases by 25% compared to traditional Fourier Transform (FT) analysis; moreover, the error in FFT analysis compared to experimental results is quite small, less than 2%. This shows that FFT is a suitable method to identify sensitive characteristics in evaluating changes in the mechanical properties. When FFT is combined with the discrete model, results are much better than those of several existing approaches. For the last idea, the manuscript applies deep learning (FFT-deep learning) in the noise reduction process for the original data. This makes the results much more accurate than in previous studies. The results of this research are shown through the monitoring of spans of the Saigon Bridge—the biggest and most important bridge in Ho Chi Minh City, Vietnam—during the past 11 years. The correspondence between the theoretically obtained result and the experimental one at the Saigon Bridge suggests a new area for development in evaluating and forecasting structural changes in the future.

**Keywords** Fast Fourier Transform (FFT) · Fourier Transform (FT) · Structured discrete models · Structural health monitoring · Deep learning

## Introduction

Viewpoints on evaluation of structural changes are usually put forward for two main reasons: a change in the overall stiffness of a load-bearing structure ( $K$ ) and a loss of binding energy of the material ( $c$ ) in that structure. At present, there are many different research approaches to evaluate the change in structures under vibration. However, we can divide those researches into two groups based on their

approaches: structured modeling and non-structured modeling. The first kind focuses on the modeling method as well as the load-bearing state of structures. This is to design a general model harmonizing theory and practice in monitoring changes in the mechanical properties of structures. Therefore, these researches employ the method to determine and forecast any possible corruption processes happening to the structure. However, changes in the model's mechanical properties are shown in different forms, such as cracks, damages, chronological deterioration or physico-chemical factors from the external environment. Therefore, researches following this tendency conclude that changes in the mechanical properties affect the stiffness of structures (overall stiffness— $K$ ). In other words, the overall stiffness directly affects the load-bearing capacity of structures in its mechanical reaction. When this happens, changes in the

✉ Thanh Q. Nguyen  
nguyenquangthanh@tdmu.edu.vn

<sup>1</sup> Faculty of Engineering and Technology, Thu Dau Mot University, Thủ Dầu Một, Bình Dương, Vietnam

<sup>2</sup> Thu Dau Mot University, Thủ Dầu Một, Bình Dương, Vietnam

mechanical characteristics of structures are defined by attenuation of stiffness, which is shown by changes in geometric dimension, geometric shape or the structure of the material [1–6]. Researchers usually model the attenuation of stiffness in load-bearing structures by cracks, gashes or other damages. In detail, the researches delve into analyzing its shape (type), such as horizontal cut, vertical cut, or cut in depth, and its detailed geometric shape of defect in the structure, such as round cut, oval cut, or oblique cut. The prominent advantage of these researches is that they give us a relatively accurate result of the relation between the reactions of a mechanical system to each type of damage (each type of structural change) and they can forecast occurrence as well as the development of these changes. The second approach delves into the general model of structures and evaluates changes of these structures by chronological deterioration or by creating damages. Accordingly, the most prominent group of researchers in this field recently includes Haugen [7], Vantadori [8, 9] and Nadeem [10–12]. The authors used fatigue as a method to evaluate changes in the mechanical characteristics of structures. This group also proposed other methods to detect and monitor the changes of structures [13–16]. Apart from monitoring changes in the mechanical characteristics using fatigue phenomena [17], Mahdi Heydar [18, 19] also assessed mechanical characteristics by creating specific damages. Furthermore, many researches have aimed at increasing the sensitivity of a signal through algorithms, such as statistical methods [20, 21], combination with optimization algorithms [22–25], combination with algorithms of artificial neural networks [26–28], combination with wavelet analysis [29, 30], or combination with the neuron-fuzz technique [23, 31] and artificial neural network algorithms [32, 33]. However, increasing the sensitivity of a signal leads to a rise in interference and a deviation in the results. Therefore, almost all the results from the above researches do not completely match with reality.

Our first idea is to employ the discrete model, which is completely different from the finite element model (FEM) and other structural discretization methods. As this method only discretizes the mechanical properties of structures with fewer degrees of freedom, the errors reduce and the results are close to the real ones. Analyzing structures using elements that are too small may lead to greater discrepancies and fail to fully display mechanical properties of original structures. The discretizing method in this research not only reduces the degree and time of calculation, but also retains all the mechanical properties of the original structure. Moreover, this paper is able to simultaneously evaluate two components affecting mechanical properties—which are overall stiffness and damping coefficient—during vibration. Focusing on only one of these components, previous researches are unable to correctly demonstrate original mechanical properties since the remaining component is often assumed

to be constant during the structure's operation. While these previous researches do not have high applicability, the newly proposed model provides an alternative potential in structural modeling.

The next contribution of this research is to use Fast Fourier Transform (FFT) analysis to increase the sensitivity of the signal and reduce errors [15, 23]. Other analytical methods are often characterized by too many calculation steps and affected by noise from the signal. FFT simplifies calculations and produces more accurate results as it is less affected by noise or calculative errors. To evaluate changes in the mechanical properties of structures, this research uses vibrational characteristics, forming a relation with the evaluating parameters. We have verified the theoretical background through continuous structural health monitoring of the Saigon Bridge's spans over 11 years. Changes in the structure of the span were complex, with variations in both the overall stiffness ( $K$ ) and the dampening coefficient ( $c$ ) during operation; furthermore, the transportation on the bridge led to much noise in the collected signals. Thus, previous models have not been able to meet the given demand. The results of this research will be a foundation to predict and forecast structural damage in the future. This manuscript is divided into four sections as follows: the first section introduces an overview of previous studies related to the manuscript. The second section builds theoretical models with the highlight being the training process of the manuscript by input parameters of the deep learning model. The third section presents the results obtained from the theoretical model built in the second section. The highlight of this section is the results obtained from the Saigon Bridge during an 11-year follow-up by continuous structural health monitoring systems. In addition, the results from the manuscript were compared with many studies by Mahdi et al. [35]. The last section shows the most striking results obtained during the research process.

## Theoretical Background

### A Novel Approach Using the Structured Discrete Model

The structured discrete model shall be applied to many actual targets. However, within this research, the investigated targets are the models of the bar or beam type with bend load as shown in Fig. 1. The structured discrete model is the most popular model in actual calculations. According to this model, bar or beam systems are consecutive mechanical systems and have infinite degrees of freedom. Theoretically, every point of an object sufficiently shows the mechanical characteristics of a structure, including elasticity (through overall stiffness of structures) and damping (through changes

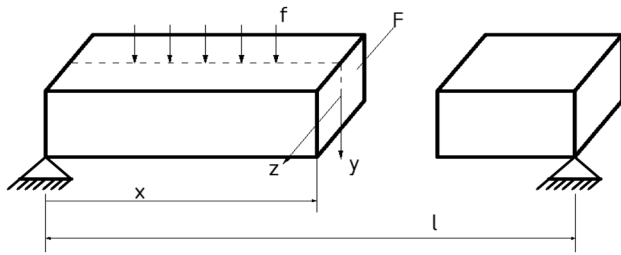


**Fig. 1** Modeling the discrete process of a structure in flat transverse bending status

in the mechanical characteristics of the material). However, actual investigation results show that beam vibration has only finite degrees of freedom, which means flat section views vibrate evenly, and then gather to a block form and vibrate as an absolute solid object. Therefore, using the discrete approach under the FEM model or other wire-frame model does not show the basic nature of structures in reality. From the above conclusion, this draft models beam structure into one discrete system, and this system still ensures the mechanical characteristics of the structures and the characteristics of the materials.

In Fig. 1,  $f$  denotes external forces;  $F$  is the section area;  $z$ ,  $y$  are the center inertia axis system of the section area  $F$ ;  $x$  is the coordinate of the section; and  $l$  is the length of the beam.

When applying this discrete model in a particular calculation, the draft offers specific proposals to evaluate the changing process of structural mechanical characteristics. The characteristics of load bearing and deformation of structures suffering a flat transverse bend (the beam) are shown as follows:

- For the act of external forces, the external force system must be placed on the center inertia flat surface containing the  $y$  axis, and simultaneously perpendicular to the  $z$  axis. The external force system does not cause the internal forces that are perpendicular to the section area.
- The deformations in the structure must comply with the flat section axiom and the vertical layer axiom. These axioms support the proposals in the draft by allowing modeling points within the section area that are perpendicular to the bar axis before deformation. When the bar is deformed, it moves like a group of points of a one solid. Besides the above axioms, a test from this research shows that in the deformation state of the beam, the section area is always perpendicular to the tangent line of the bar axis.
- Energy loss always happens when the beam vibrates. It is shown as damped vibration.

The structured discrete model can be shown by models of the following types: one degree of freedom in Fig. 2;

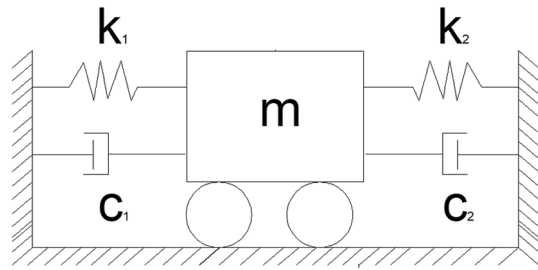


**Fig. 2** Discrete mechanical system of one degree of freedom

two degrees of freedom in Fig. 3; three degrees of freedom in Fig. 4. The common characteristics of these models are shown by two elements: the overall stiffness ( $K$ ) and the overall damping ( $c$ ).

To use the discrete model, the selected mechanical system must ensure that the number of degrees of freedom suits the reaction of the corresponding structure. When the structure ensures the mechanical characteristics, the mechanical system must ensure elasticity and damping. In this research, we use discrete mechanical systems while ensuring the above-mentioned components. This is the main criterion in assessing changes in the mechanical characteristics of structures. In case the mechanical system suffers external forces acting on it, the differential equation showing the vibration process has the general form as in Eq. (1):

$$[M]\ddot{\vec{q}} + [c]\dot{\vec{q}} + [k]\vec{q} = \vec{F}(t) \quad (1)$$

in which  $[M]$  is the mass matrix,  $[c]$  is the damping matrix,  $[k]$  is the stiffness matrix,  $\vec{q}$  is the displacement vector or generalized coordinate, and  $\vec{F}(t)$  is the acting force vector.

The method to solve the differential Eq. (1) is shown for each structure as below:

- For the mechanical characteristics of structures shown by one degree of freedom, the vibration equation of the mechanical system is depicted in the following equation:

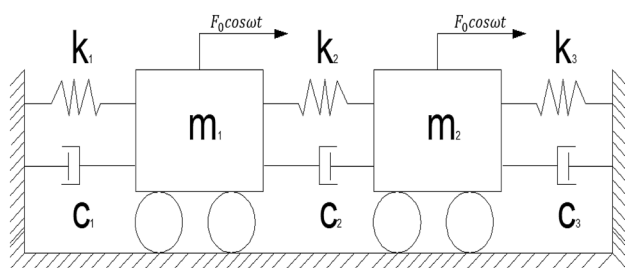


**Fig. 3** Discrete mechanical system of two degrees of freedom

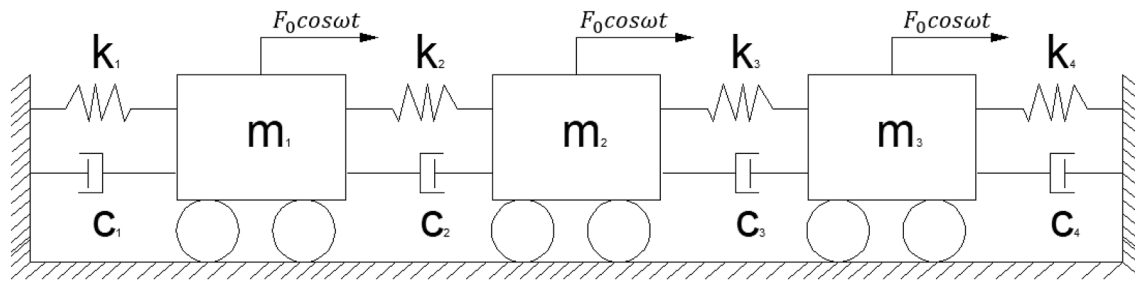


**Fig. 4** Discrete mechanical system of three degrees of freedom

$$A \{ (k_1 + k_2 - mp_n^2) \cos(p_n t - \phi) - (c_1 + c_2)p_n \sin(pt - \phi) \} = F_0 \cos \omega t. \quad (2)$$

- For the mechanical characteristics of structures shown by two degrees of freedom, the vibration equation of the mechanical system is shown in the following equation:

$$\begin{Bmatrix} A_1 \\ A_2 \end{Bmatrix} = \begin{pmatrix} (-p_n^2 m_{11} + ip_n c_{11} + k_{11}) & (-p_n^2 m_{12} + ip_n c_{12} + k_{12}) \\ (-p_n^2 m_{21} + ip_n c_{21} + k_{21}) & (-p_n^2 m_{22} + ip_n c_{22} + k_{22}) \end{pmatrix}^{-1} \begin{Bmatrix} F_{10} \\ F_{20} \end{Bmatrix}. \quad (3)$$

- For the mechanical characteristics of structures shown by three degrees of freedom, the vibration equation of the mechanical system is expressed in the following equation:

$$\begin{Bmatrix} A_1 \\ A_2 \\ A_3 \end{Bmatrix} = \begin{pmatrix} (-p_n^2 m_{11} + ip_n c_{11} + k_{11}) & (-p_n^2 m_{12} + ip_n c_{12} + k_{12}) & (-p_n^2 m_{13} + ip_n c_{13} + k_{13}) \\ (-p_n^2 m_{21} + ip_n c_{21} + k_{21}) & (-p_n^2 m_{22} + ip_n c_{22} + k_{22}) & (-p_n^2 m_{23} + ip_n c_{23} + k_{23}) \\ (-p_n^2 m_{31} + ip_n c_{31} + k_{31}) & (-p_n^2 m_{32} + ip_n c_{32} + k_{32}) & (-p_n^2 m_{33} + ip_n c_{33} + k_{33}) \end{pmatrix}^{-1} \begin{Bmatrix} F_{10} \\ F_{20} \\ F_{30} \end{Bmatrix} \quad (4)$$

in which  $A_i$  is the vibration amplitude for a number  $i$  of structures, and  $p_n$  is the natural frequency.

The root of Eqs. (2, 3 and 4) can be written as depicted in Eq. (5), and this is to show the mechanical characteristics of structures during the vibration process with two main components, vibration amplitude and natural vibration frequency:

$$q(t) = A_0 e^{-\zeta p_n t} \cos(\sqrt{1 - \zeta^2} p_n t - \Phi_0). \quad (5)$$

However, there is always energy loss (due to the changes in material characteristics) during the operation of structures. To assess this change, the research inserts a damping component into the model to accurately reflect its mechanical characteristics.  $p_d$  is the value of the damping vibration frequency expected from theory. This is the frequency of vibration of structures under the energy loss of damping  $c$  as shown in the following equation:

$$p_d = \sqrt{1 - c^2} p_n \Leftrightarrow q(t) = A_0 e^{-cp_n t} \cos(p_d t - \Phi_0). \quad (6)$$

In fact, we can determine the damping coefficient  $c$  by experimental methods based on the damping vibration graph of the mechanical system. Symbols  $q_1, q_2$  are two adjacent peaks of damped vibration as shown in Fig. 5. The time

recorded at the two peaks are  $t_1, t_2$ . Then, we establish the ratio below:

$$\frac{q_1}{q_2} = \frac{A e^{-\zeta p_n t_1} \cos(p_d t_1 - \Phi_0)}{A e^{-\zeta p_n t_2} \cos(p_d t_2 - \Phi_0)} \quad (7)$$

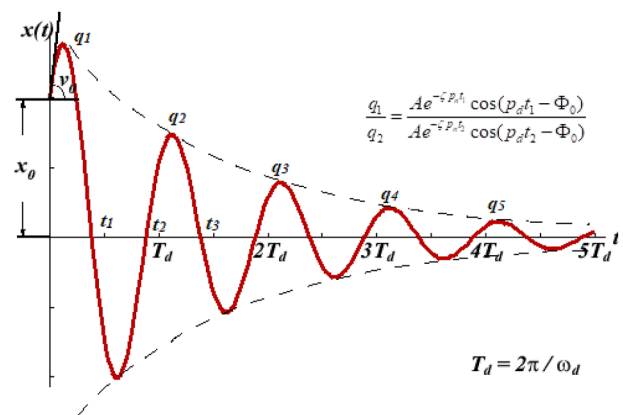


**Fig. 5** Determining damping coefficient by the experimental method

As  $q_1, q_2$  are two adjacent peaks of the above graph, so  $t_2 = t_1 + T_d$

$$p_d t_2 = p_d t_1 + p_d T_d = p_d t_1 + 2\pi. \quad (8)$$

According to Eq. (8):

$$\cos(p_d t_2 - \Phi_0) = \cos(p_d t_1 + 2\pi - \Phi_0) = \cos(p_d t_1 - \Phi_0). \quad (9)$$

Then, the ratio in Eq. (7) becomes:

$$\frac{q_1}{q_2} = e^{cp_n T_d}. \quad (10)$$

Given logarithm base  $e$  of the above equation, we suppose that symbol  $\delta$  is the logarithmic decrement and have the  $\delta$  expression as below:

$$\delta = \ln \frac{q_1}{q_2} = cp_n T_d \quad (11)$$

Provided that  $\begin{cases} T_d = \frac{2\pi}{p_d} \\ p_d = p_n \sqrt{1 - c} \end{cases}$  then the final expression becomes:

$$\delta = \frac{2\pi}{\sqrt{1 - c^2}}. \quad (12)$$

If  $c \ll 1$  then the above expression can also be written as:

$$\delta \approx 2\pi c \quad (13)$$

From Eq. (13), we can calculate  $c$  by the equation below:

$$c = \frac{\delta}{\sqrt{(2\pi)^2 + \delta^2}}. \quad (14)$$

From Eq. (14), we can estimate  $c$ :

$$c \approx \frac{\delta}{2\pi}. \quad (15)$$

To enhance the accuracy in determining the value of  $c$ , we take two peaks that are a distance from each other of  $m$  cycles in the graph instead of two adjacent peaks. Then, the ratio between  $q_1$  and  $q_m$  is:

$$\frac{q_1}{q_{1+m}} = \frac{q_1}{q_2} \cdot \frac{q_2}{q_3} \cdots \frac{q_m}{q_{1+m}} \quad (16)$$

From Eqs. (14) and (16), we derive:

$$\delta = \frac{1}{m} \ln \left( \frac{q_1}{q_{m+1}} \right) \quad (17)$$

However, the value of the damping coefficient  $c$  in the calculation usually varies, as the actual attenuation process usually differs. The damping signal segments are unclearly shown in Fig. 6. Therefore, to enhance the accuracy of this coefficient, the research uses the FFT to reduce the quantity of interference and increase the stability of the signal.

## Fast Fourier Transform (FFT)

When a load-bearing structure vibrates, its condition can be studied to assess its actual mechanical characteristics. Normally, to evaluate the vibration frequency and amplitude of structures, researchers use the Fourier Transform (FT) of the input signal function  $x_k(t)$  and  $x_l(t)$ . The shortcomings of FT are the large number of calculations and the large effect of signal interference. If the number of discrete values is  $N$  in the formula of FT, we have to take  $N^2$  multiplications and  $N^2$  summations of complex numbers,

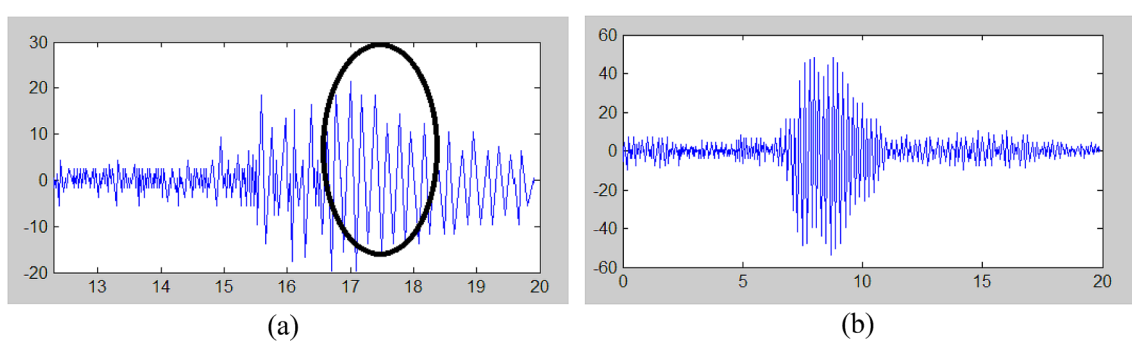


**Fig. 6** The unclearly shown damping signal segments

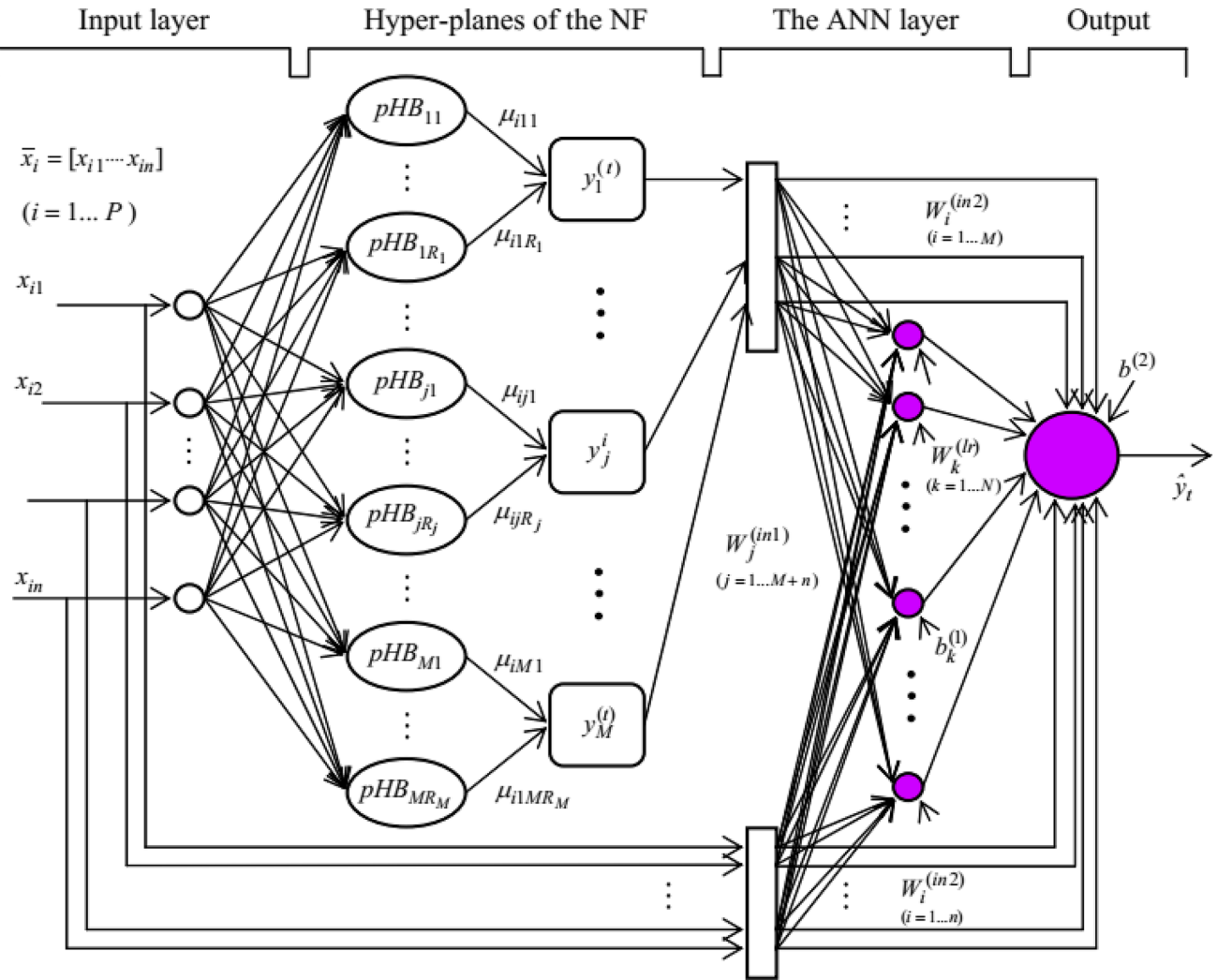


**Fig. 7** Deep learning training model [36]

so the total is  $2N^2$  arithmetic calculations. If  $N$  is large (necessary when high accuracy is preferred), the signal processing will encounter a major problem. In order to simplify the calculations using FT, the draft uses a special algorithm, which allows reduction in the number of necessary calculations. These algorithms are called Fast Fourier Transform (FFT):

$$\begin{aligned} X_k(\omega) &= \int_{-\infty}^{+\infty} x_k(t)e^{-i\omega t} dt \\ X_l(\omega) &= \int_{-\infty}^{+\infty} x_l(t)e^{-i\omega t} dt = \int_{-\infty}^{+\infty} x_l(t+\tau)e^{-i\omega(t+\tau)} dt \end{aligned} \quad (18)$$

On the contrary,  $x_k(t)$  and  $x_l(t)$  can also be determined through reverse FFT:

$$\begin{aligned} x_k(t) &= \frac{1}{2\pi} \int_{-\infty}^{+\infty} X_k(\omega)e^{i\omega t} d\omega \\ x_l(t+\tau) &= \frac{1}{2\pi} \int_{-\infty}^{+\infty} X_l(\omega)e^{i\omega(t+\tau)} d\omega. \end{aligned} \quad (19)$$

Actually, the collected responses of  $x_k(t)$  and  $x_l(t)$  are two samples of ergodic processes. It means that both  $x_k(t)$  and  $x_l(t)$  satisfy requirements of a random process and ensure the stopping characteristic in collecting the signal. Then, the mathematical expectation of  $x_k(t)$  and  $x_l(t)$  during sample collecting time  $T$  is shown in the following equation:

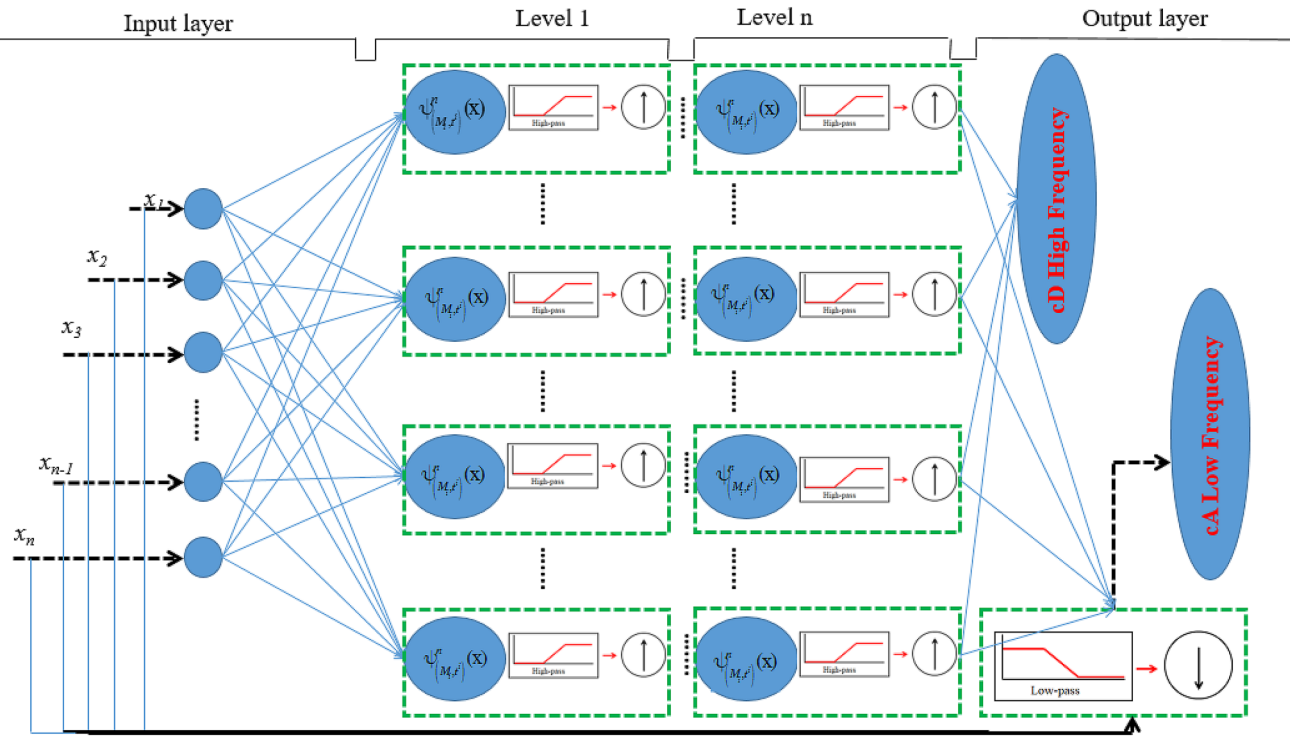


**Fig. 8** Deep learning training model present [34]

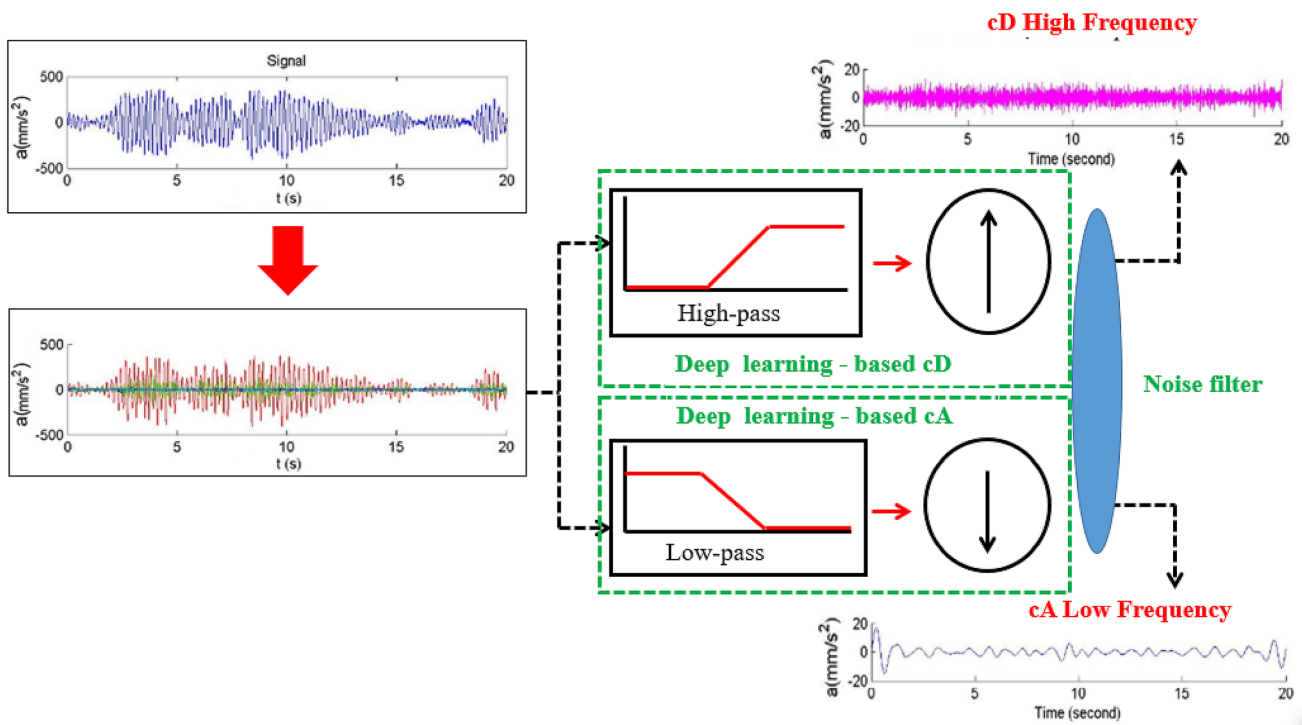


**Fig. 9** The original data training of the present model [34]

$$\begin{aligned}\langle x_k(t), x_l(t + \tau) \rangle &= \frac{1}{T} \int_0^T x_k(t) x_l(t + \tau) dt \\ \langle x_k(t), x_l(t + \tau) \rangle &= \frac{1}{T} \int_0^T x_k(t) \left\{ \frac{1}{2\pi} \int_{-\infty}^{+\infty} X_l(\omega) e^{i\omega(t+\tau)} d\omega \right\} dt \\ \langle x_k(t), x_l(t + \tau) \rangle &= \frac{1}{2\pi} \frac{1}{T} \int_0^T \left\{ \int_{-\infty}^{+\infty} x_k(t) e^{i\omega t} dt \right\} d\omega \\ \langle x_k(t), x_l(t + \tau) \rangle &= \frac{1}{2\pi} \frac{1}{T} \int_0^T X_k^*(\omega) X_l(\omega) e^{i\omega t} d\omega\end{aligned}\quad (20)$$

in which  $X_k^*(\omega)$  is the conjugate form of  $X_k(\omega)$ , and  $R_{kl}(\tau)$  is recalculated by the following equation:

$$\begin{aligned}R_{kl}(\tau) &= E[x_k(t)x_l(t + \tau)] \\ R_{kl}(\tau) &= \frac{1}{2\pi} \int_{-\infty}^{+\infty} \lim_{T \rightarrow \infty} E\left[\frac{1}{T} X_k^*(\omega) X_l(\omega)\right] e^{i\omega t} d\omega.\end{aligned}\quad (21)$$

Through Fourier transform of the input stimulus force function  $f(t)$ , the frequency response is shown in the following equation:

$$F(\omega) = \{F_1(\omega) F_2(\omega) \dots F_n(\omega)\}^T \quad (22)$$

The  $j$ th position of the frequency response matrix is expressed as follows:

$$H_j(\omega) = \{H_{j1}(\omega) H_{j2}(\omega) \dots H_{jn}(\omega)\} \quad (23)$$

Therefore,  $X_k(\omega)$  and  $X_l(\omega)$  can be rewritten by Eqs. (22) and (23):

$$\begin{aligned}X_k(\omega) &= H_k(\omega) F(\omega) \\ X_l(\omega) &= H_l(\omega) F(\omega)\end{aligned}\quad (24)$$

We apply Eq. (24) into Eq. (21), and the cross-correlation coefficient of the power spectrum between  $x_k(t)$  and  $x_l(t)$  can be expanded as below:

$$R_{kl}(\tau) = \frac{1}{2\pi} \int_{-\infty}^{+\infty} \lim_{T \rightarrow \infty} E\left\{\frac{1}{T} [H_k(\omega) F(\omega)]^* H_l(\omega) F(\omega)\right\} e^{i\omega\tau} d\omega \quad (25)$$

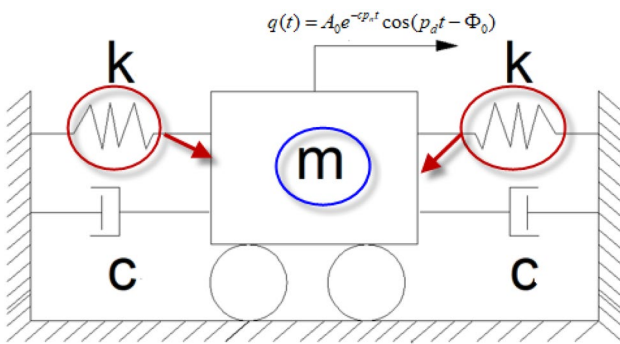


**Fig. 10** The one degree of freedom discrete system with changing  $K$

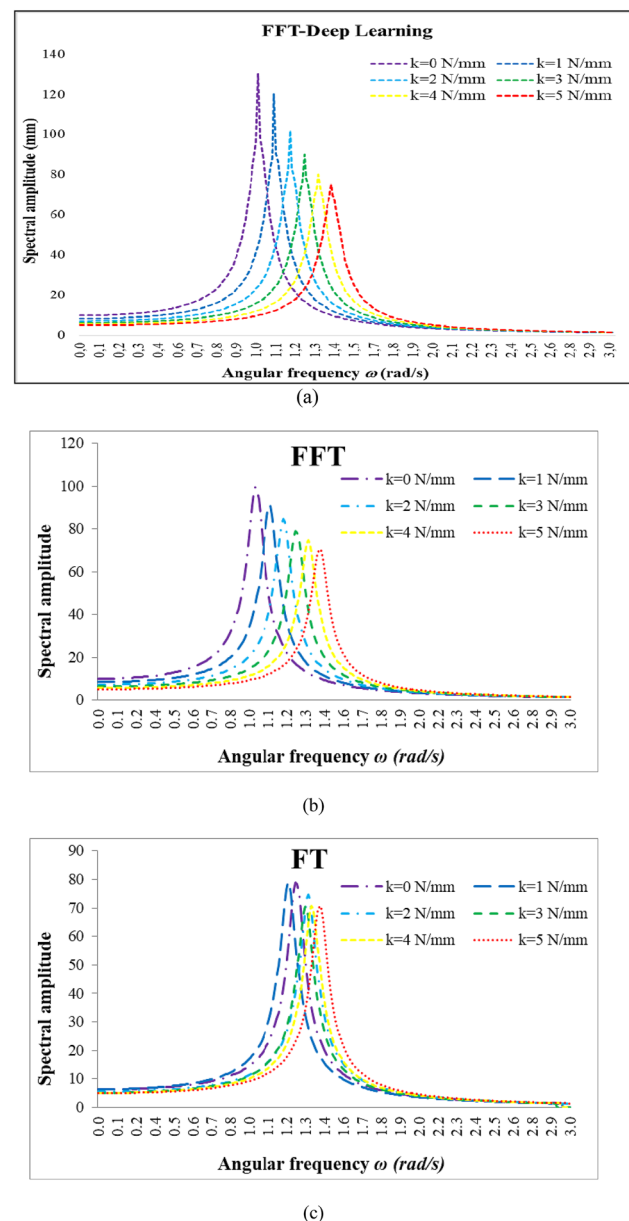


**Fig. 11** Spectral amplitude changes when stiffness varies

Therefore,  $r_{kl}$  is depicted in the following equation:

$$\begin{aligned}r_{kl} &= |R_{kl}(\tau_l)| \\ &= \frac{1}{2\pi} \int_{-\infty}^{+\infty} \lim_{T \rightarrow \infty} E\left\{\frac{1}{T} |[H_k(\omega) F(\omega)]^* H_l(\omega) F(\omega)|\right\} e^{i\omega\tau_l} d\omega\end{aligned}\quad (26)$$

If the stimulus force function  $F(\omega)$  in Eq. (26) has a specific form and  $\tau_l$  is constant, then  $r_{kl}$  ( $l = 1, 2, 3, \dots, n$ ) is dependent only on the frequency response matrix of the structures.

## Building a Deep Learning Model

The training parameters consisting of bias and weight of deep learning should be presented as shown in Fig. 7:

Step 1: Select Wavelet Candidates: It can be described by a set of input signals

$$f(t) = A_J + \sum_{j \leq J} D_j = \sum_{i=1}^n K^i = \sum_{i=1}^n [X_i, Y_i, 0]. \quad (27)$$

Step 2: Select signal analysis:  $\mathbf{K}^i$ : If  $x_1$  is  $[X_1, Y_1, 0]$  and  $x_2$  is  $[X_2, Y_2, 0]$ , and ... and  $x_{n-1}$  is  $[X_{n-1}, Y_{n-1}, 0]$ , and  $x_n$  is  $[X_n, Y_n, 0]$ , the original signal is analyzed by the matrix  $[\mathbf{K}]$  as shown in Eq. (28) and Fig. 8.

$$\begin{aligned} [\mathbf{K}] &= [\mathbf{K}^i]^T = [x_1 \ x_2 \ \dots \ x_{n-1} \ x_n]^T \\ &= \begin{bmatrix} X_1 & Y_1 & 0 \\ X_2 & Y_2 & 0 \\ \dots & \dots & \dots \\ X_{n-1} & Y_{n-1} & 0 \\ X_n & Y_n & 0 \end{bmatrix} \end{aligned} \quad (28)$$

in which  $\mathbf{K}^i$  is the  $i$ th rule,  $(1 \leq i \leq n)$  and  $x_i$  ( $1 \leq i \leq n$ ) are the input variables of  $X_i$  and  $Y_i$ .

Then,  $\hat{y}_i = \sum_{i=1}^{T_i} \omega_{(M_i, t^i)} \psi_{(M_i, t^i)}^n(x)$ , with  $M \in Z$ ;  $t^i \in \mathbb{R}$  and  $\omega_{(M_i, t^i)} \in \mathbb{R}$ ;  $x \in \mathbb{R}^*$  ( $\mathbb{R}$  is a real number; however, in this case study, we remove the number of value zero in  $\mathbb{R}$  that is called  $\mathbb{R}^*$ ), where  $T_i$  is the total number of

deflection signals in damage states and different fault states.  $y_i$  is the output of the deep learning training model,  $y_{(M_i, t^i)}^n(x)$  is the same dilation value as  $M \in Z$ , and  $t^i \in \mathbb{R}$  indicates the symbols of translation parameter  $[t^i] = t_1^i, t_2^i, \dots, t_{n-1}^i, t_n^i$ .

Step 3: Filter signal components: Based on the previous description, we obtain the following:

$$\begin{aligned} y_{(M_i, t^i)}^n(x) &= 2^{\frac{M_i}{2}} y^i(2^{M_i} x - t^i) \\ &= \prod_{i=1}^n 2^{\frac{M_i}{2}} y^i(2^{M_i} x_i - t_n^i) \text{ with } M \in Z; t_n^i \in \mathbb{R} \end{aligned} \quad (29)$$

and

$$\hat{\mu}_i(x) = \frac{\mu_i(x)}{\sum_{i=1}^n \mu_i(x)}. \quad (30)$$

The output of the deep learning training model is as follows:

$$\hat{y} = \frac{\sum_{i=1}^n \mu_i(x) \hat{y}_i}{\sum_{i=1}^n \mu_i(x)} = \sum_{i=1}^n \hat{\mu}_i(x) \hat{y}_i. \quad (31)$$

Step 4: End of algorithm: we use the training algorithm to decompose the original signals into seven signal layers in the context of hidden layers.

The results of the original data training are shown in Fig. 9.

**Table 1** Natural frequency value of mechanical system

Stiffness	K	0.95 K	0.9 K	0.85 K	0.8 K	0.75 K	0.7 K
<i>f</i> -(FFT-deep learning)							
Displacement	10.04	9.80	9.60	9.31	9.09	8.72	8.49
Velocity	10.05	9.81	9.59	9.30	9.12	8.73	8.48
Acceleration	10.06	9.81	9.57	9.29	9.10	8.72	8.47
<i>f</i> -(FFT)							
Displacement	10.04	9.87	9.59	9.30	9.05	8.77	8.44
Velocity	10.08	9.84	9.57	9.29	9.02	8.73	8.47
Acceleration	10.07	9.81	9.55	9.28	9.00	8.72	8.42
<i>f</i> -(FT)							
Displacement	10.34	10.10	9.75	9.57	9.28	9.02	8.74
Velocity	10.33	10.09	9.77	9.54	9.22	9.04	8.79
Acceleration	10.35	10.08	9.79	9.53	9.21	9.01	8.77
Finite element method (FEM)	10.06	9.79	9.53	9.24	9.02	8.70	8.40

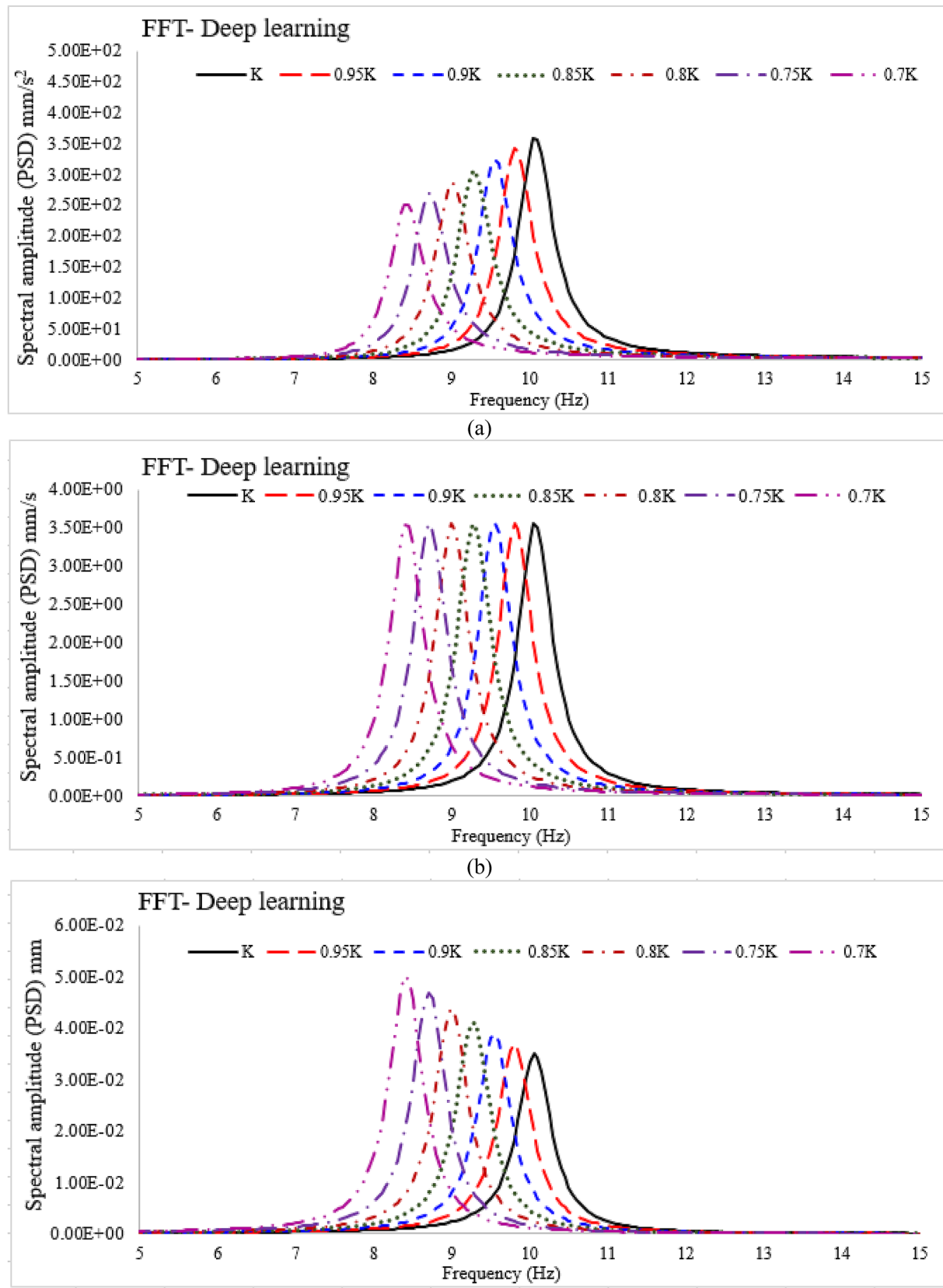


**Fig. 12** Power spectrum according to attenuation level: **a** displacement, **b** velocity, **c** acceleration

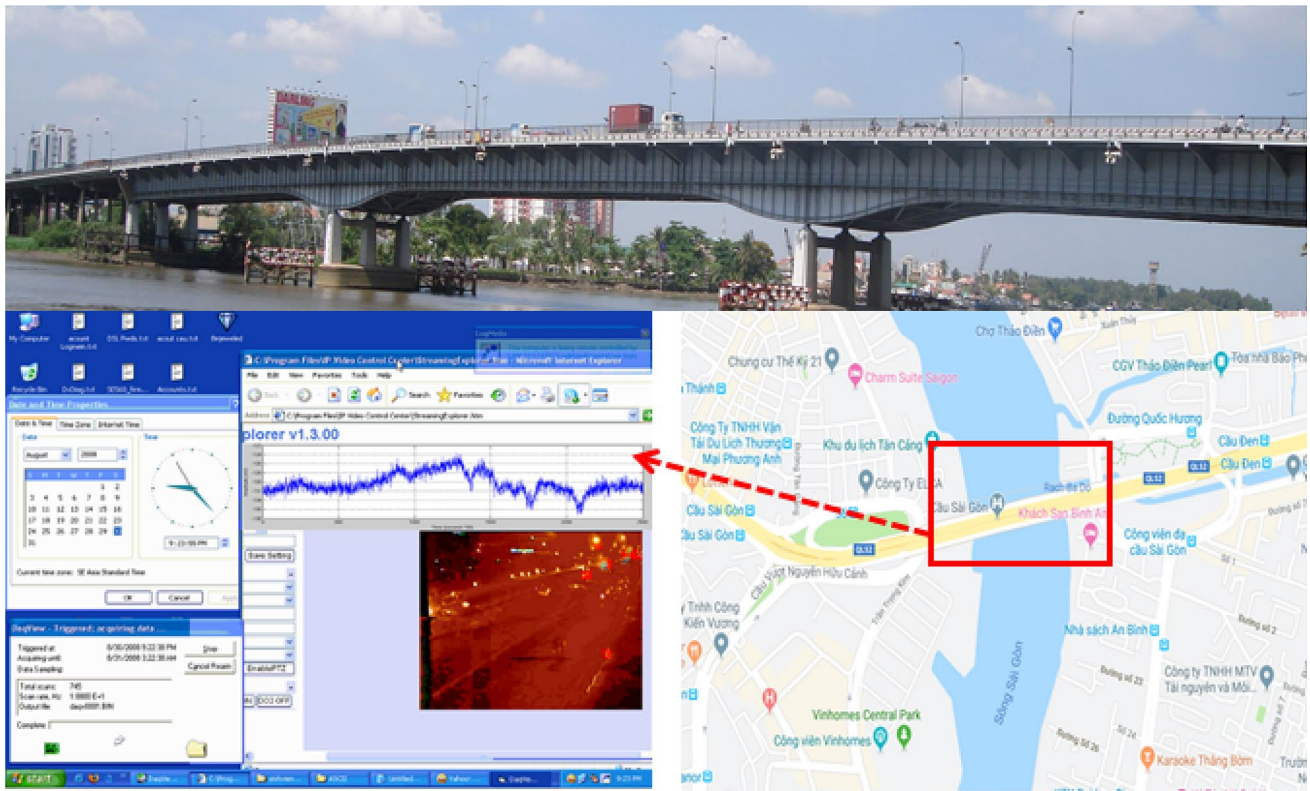


**Fig. 13** The view of Sai Gon Bridge

## Results and Discussion

### Assessment of Changes in the Mechanical Characteristics of Structures Using FFT-Deep Learning

The effect on the mechanical characteristics of structures during the vibration process is shown by two components: the stiffness of structures and the damping of materials. In the Fast Fourier Transform analysis with the combination deep learning from the original data training, these components clearly show changes in the mechanical characteristics at the frequency area where resonance occurs during the vibration process. Therefore, to fully understand this effect, the draft proposes to investigate changes in the mechanical characteristics of structures with different mechanical systems, such as those having one degree of freedom and multiple degrees of freedom. Among those, in the FFT-deep learning, changes in the system's mechanical characteristics and the attenuation in the materials' stiffness were the most evident. These results can be applied to many actual calculations in detecting and diagnosing changes in the mechanical characteristics of structures.

### The Effect of the Stiffness Component on Vibration Characteristics

To investigate the effect of the stiffness component during the vibration process, this research used a one degree of freedom discrete system, as shown in Fig. 10, with mass  $m=3$  kg, and varying stiffness with  $K=12,000$  N/m. The study proposed to change input parameters of the model, including  $K$ .

In addition, through FFT-deep learning, the draft sets forth stiffness  $k$  varying in different states. The research evaluated the effect of the structures' stiffness through measuring spectral amplitude by FFT-deep learning, as shown in Fig. 11a:

In Fig. 11, the more the stiffness attenuated, the more the vibration amplitude increased; and the maximum value of the frequency decreased. To evaluate changes in structural stiffness, researches are usually based on the structure's natural frequency during the vibration process. Throughout the frequency spectrum, changes of frequency value are relatively large. FFT-deep learning and FFT analysis (see Fig. 11a, b) show that changes in frequency value and spectral amplitude were much larger than in normal FT analysis. Specifically, the angular frequency in the spectrum analyzed

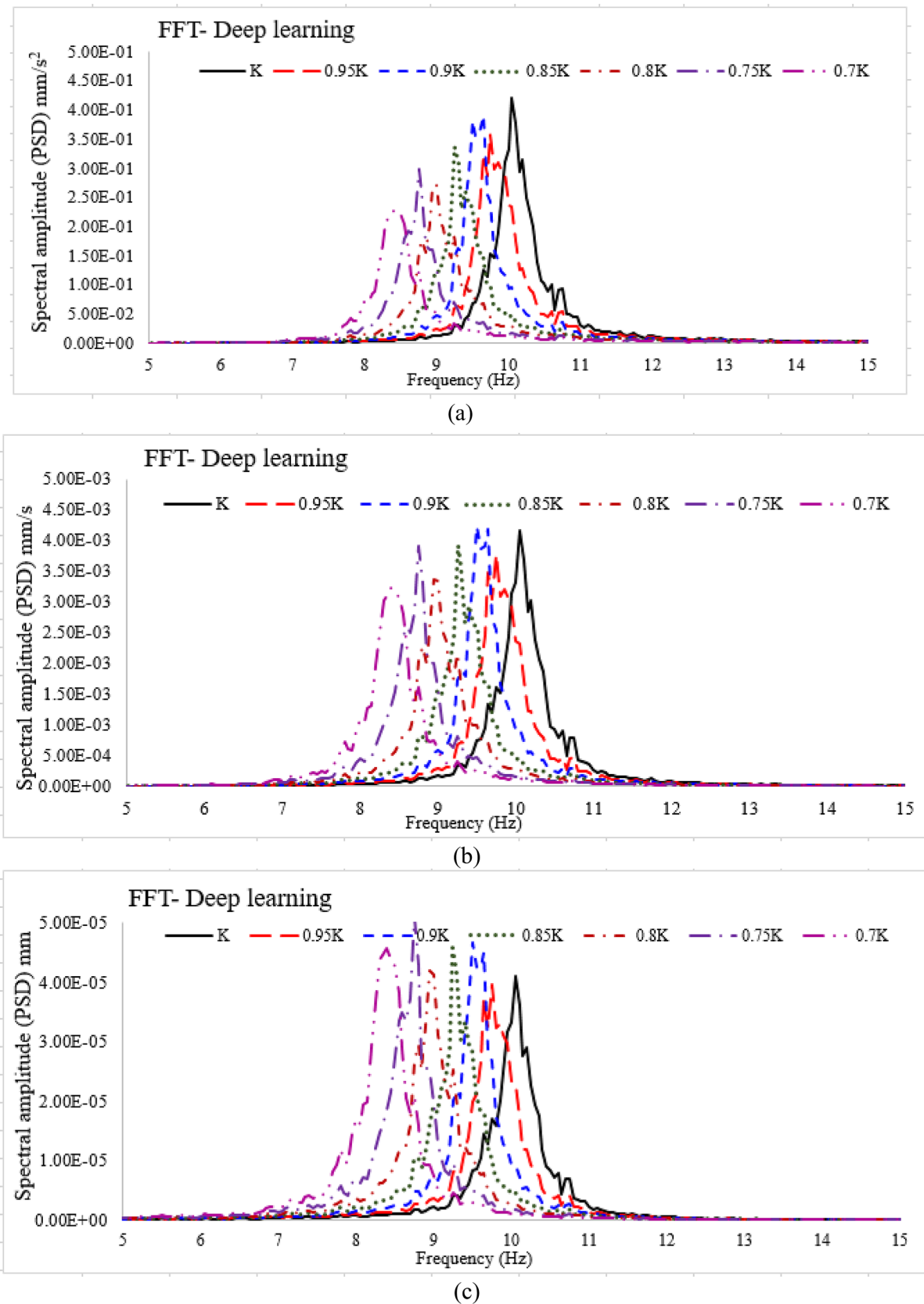


**Fig. 14** Power spectrum according to attenuation level: **a** displacement, **b** velocity, **c** acceleration of three-span Sai Gon Bridge

**Fig. 15** The relation between the changes in stiffness  $K$  of structures according to attenuation level: **a** displacement, **b** velocity, **c** acceleration with FFT-deep learning and FT

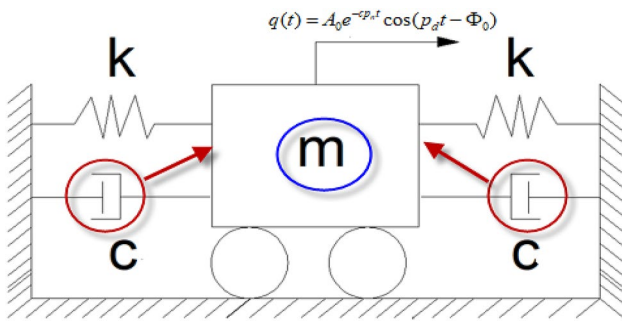
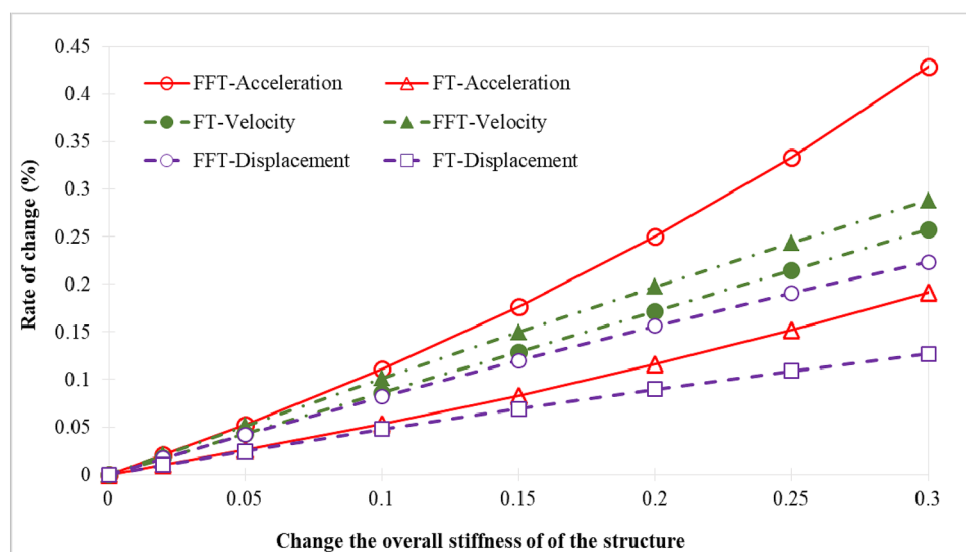


**Fig. 16** The one degree of freedom discrete system with changing c

using FFT and deep learning varied over 20% more than using FT, and the spectral amplitude varied over 15%, as shown in Fig. 11b. Therefore, the result from FFT is highly sensitive in comparison with other researches using FT. For an actual mechanical system, change in stiffness in the load-bearing structure altered the characteristics of the spectrum. Depending on each natural vibration form of the structure, the model was shown by one degree of freedom or multiple degrees of freedom. Stiffness representing the mechanical characteristics of structures varied, respectively (0%, 5%, 10%, 15%, 20%, 25%, 30%). In each circumstance, the natural frequency value was calculated using FFT-deep learning, FFT and FT. The calculation results are shown in Table 1, in which the draft investigated different forms of signals when the mechanical system suffered vibrations. The results shown include values for displacement, velocity and acceleration.

The natural frequency response is a value depending on the material characteristics of the mechanical system and the mechanical characteristics of the structures. The research shows that these characteristics formed different spectra. This research proposed to apply spectrum

characteristics to monitor the changing state of the mechanical characteristics of structures. Therefore, the application of FFT and deep learning was more efficient than using FT. In addition, depending on the signal type used for FFT and deep learning, the characteristics of the spectra were different, as shown in Fig. 12. The results show that the frequency values obtained from FFT-deep learning and FFT analysis are similar. Therefore, in this manuscript, the training process by deep learning aims to reduce noise and optimize the results. We will combine the two methods above and call on FFT analysis. However, the common mechanical characteristics of structures were shown when the stiffness of the mechanical system attenuated, and then the frequency in the response spectrum tended to move to the lower side. On the contrary, regarding the shape and spectral amplitude value, the spectrum of displacement response grew, the spectrum of velocity response stayed the same, and the spectrum of acceleration response attenuated.

Changes in the mechanical characteristics of the three-span Sai Gon Bridge were monitored for 11 years (from January 2009 to August 2019). The Saigon Bridge, known as Newport Bridge, is a bridge crossing the Saigon River, as shown in Fig. 13. The bridge has four lanes for cars and two lanes for motorcycles and bicycles. The bridge is one of the most vital gateways for vehicles traveling from northern and central Vietnam to Ho Chi Minh city.

Corresponding to the signals of displacement, velocity and acceleration, through FFT-deep learning, the research monitored changes in the mechanical characteristics in the structure during the entire operation period of the bridge span. Figure 14 shows that

- The displacement for frequency values (ranging from high frequency to low frequency) strictly complied with

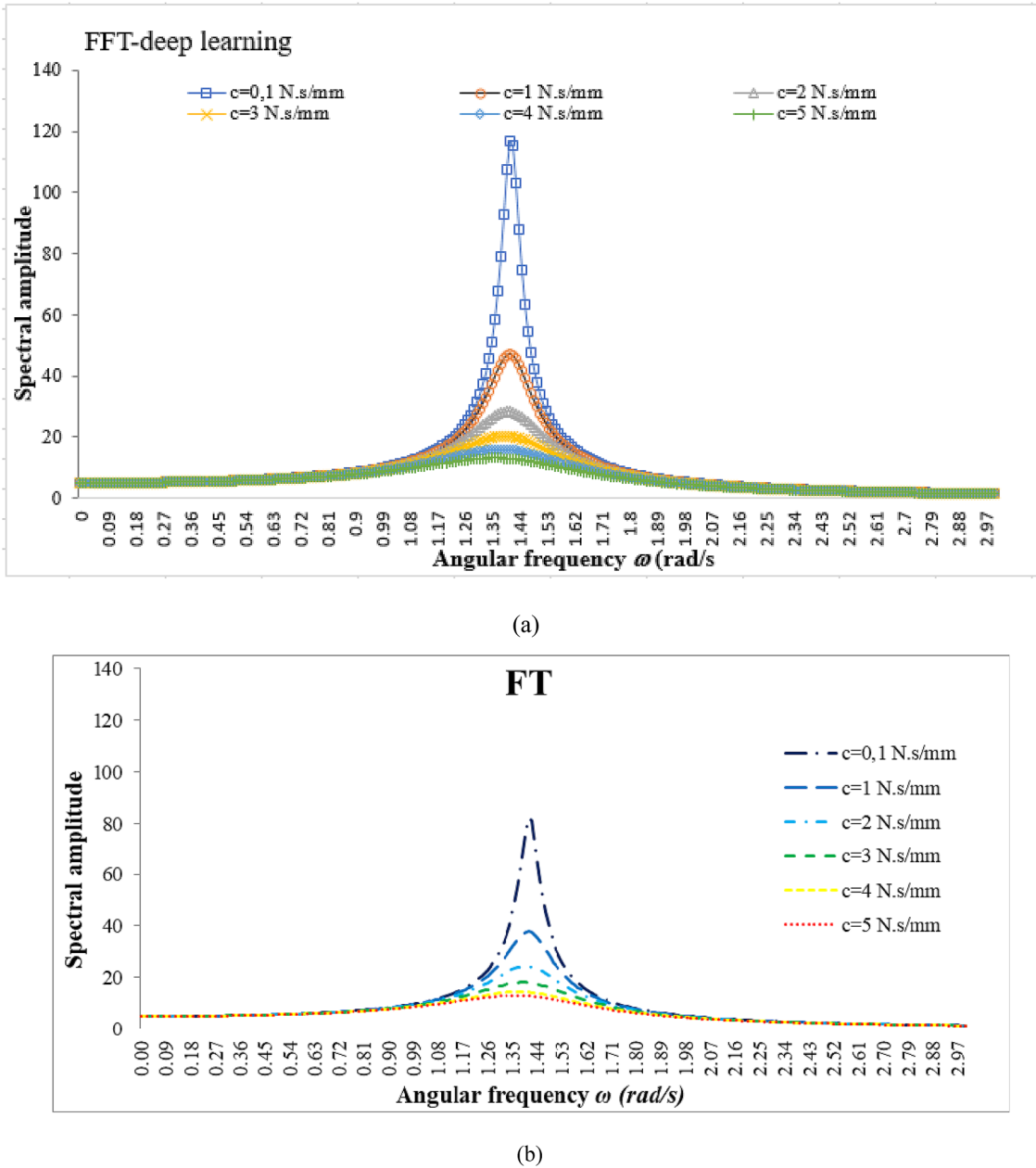


**Fig. 17** Changes in spectral amplitude when damping coefficient varies

the simulation process rule. It showed changes in the mechanical characteristics of the span during the entire monitoring period (11 years). The displacement for the natural frequency value had the same behavior for different forms of signals (displacement, velocity, and acceleration).

- In contradiction to the displacement for frequency, the amplitude of the spectrum for displacement and velocity signals was different from the simulation process, as depicted in Fig. 14. Changes in this amplitude fluctuated significantly during the entire operation period. However,

the value of the spectral amplitude analyzed from acceleration was much more efficient. It can also be explained that the displacement and velocity signals were less stable than the vibration signal.

Changes in the stiffness of structures analyzed through FFT-deep learning and FT are shown in Fig. 15. The result shows that when we combined the acceleration signal and FFT-deep learning, the sensitivity was highest. Besides, FFT-deep learning always yields more sensitive results than FT in each form of signal. It shows the possibility of

**Fig. 18** Rate of changes of maximum vibration amplitude when the mechanical characteristics vary

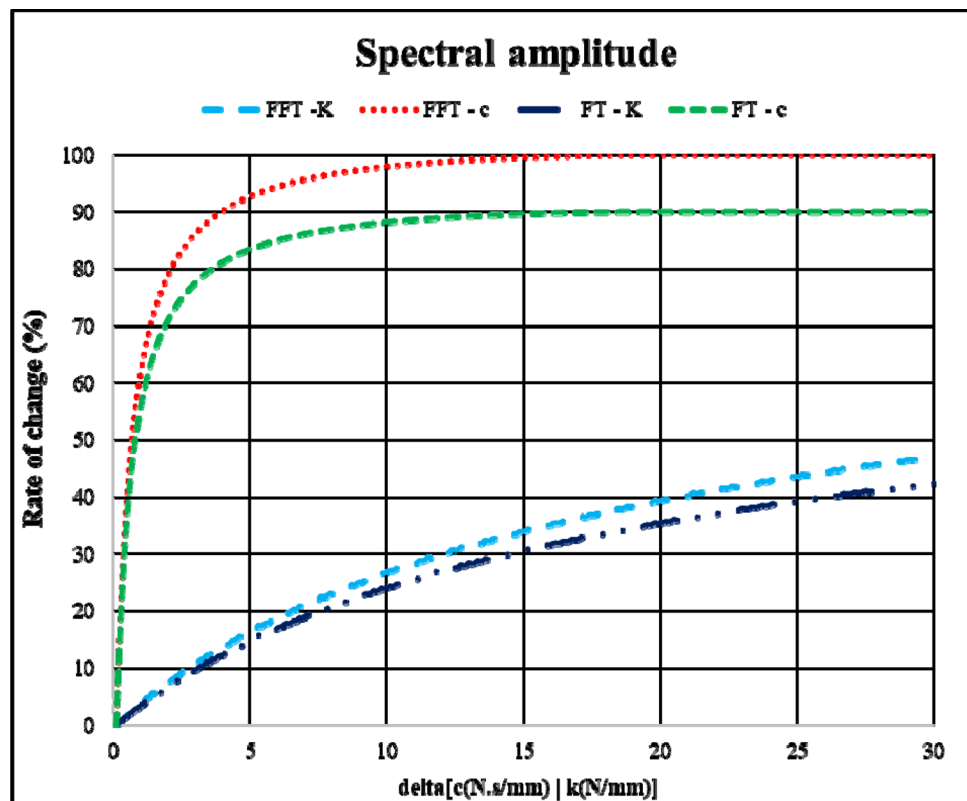


**Fig. 19** Rate of changes in resonant frequency when the mechanical characteristics vary

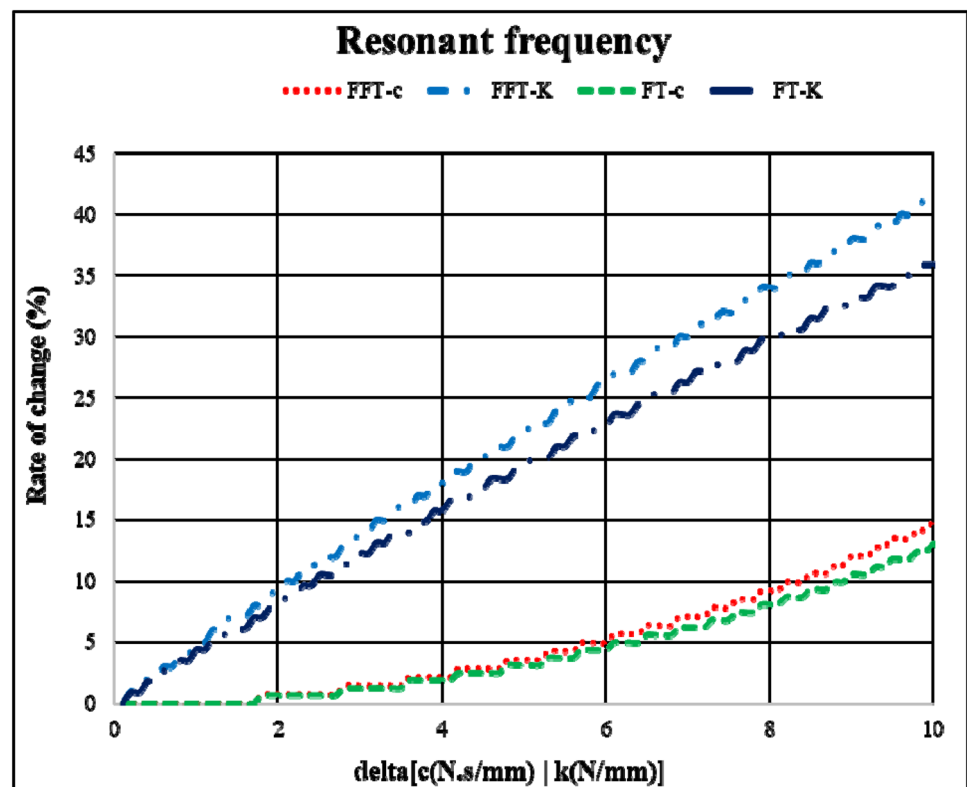


**Fig. 20** The effect of the overall damping coefficient ( $c$ ) on the mechanical characteristics of the material with two degrees of freedom model

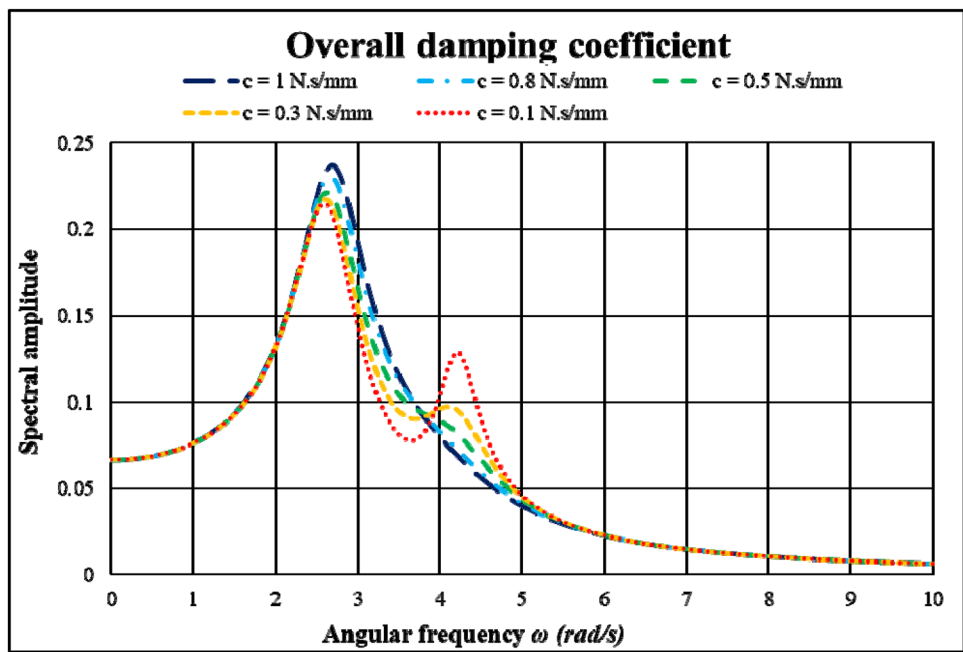
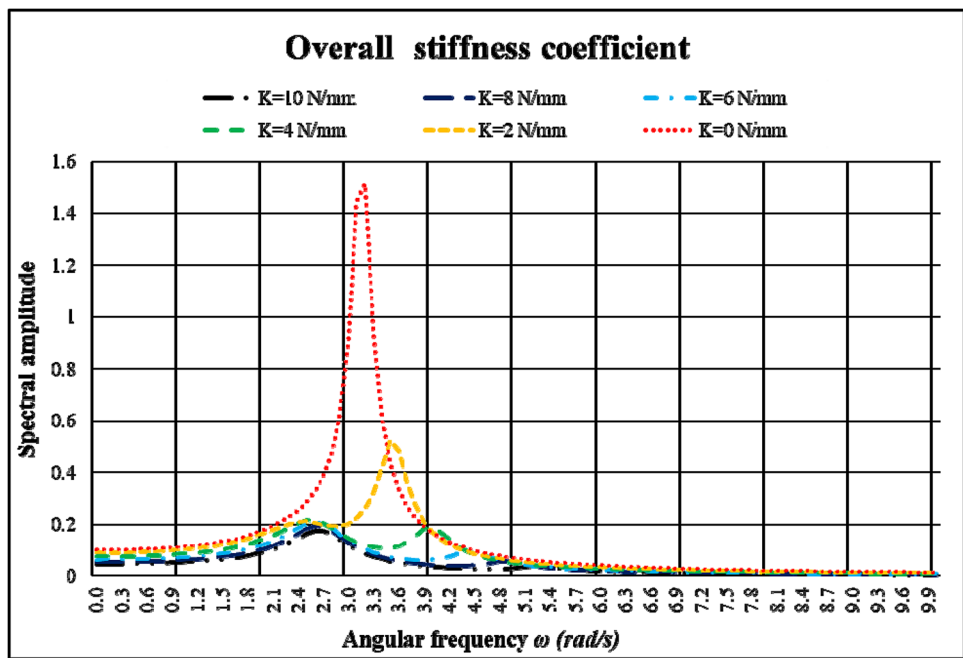


**Fig. 21** The effect of the overall stiffness ( $K$ ) on the mechanical characteristics of material with two degrees of freedom model



application of FFT-deep learning during monitoring and evaluating changes in the mechanical characteristics of structures in reality.

#### The Effect of the Damping Component on the Vibration Characteristics

To investigate the effect of the damping component during the vibration process, this research simulated the damping coefficient variable, and from that we can see the effect of

the component on the structure's mechanical characteristics. The draft also used one degree of freedom with a changing damping coefficient as shown in Fig. 16, with mass  $m = 3$  kg and damping constant  $c = 10$  Ns/m. Through FFT (see Fig. 17a) and FT (see Fig. 17b), the mechanical characteristics of the material showed a relationship with the damping component. This component then changed the shape of the vibration spectrum through the spectral amplitude and the frequency at its maximum value. The change in spectral amplitude when the damping coefficient varies is as below:

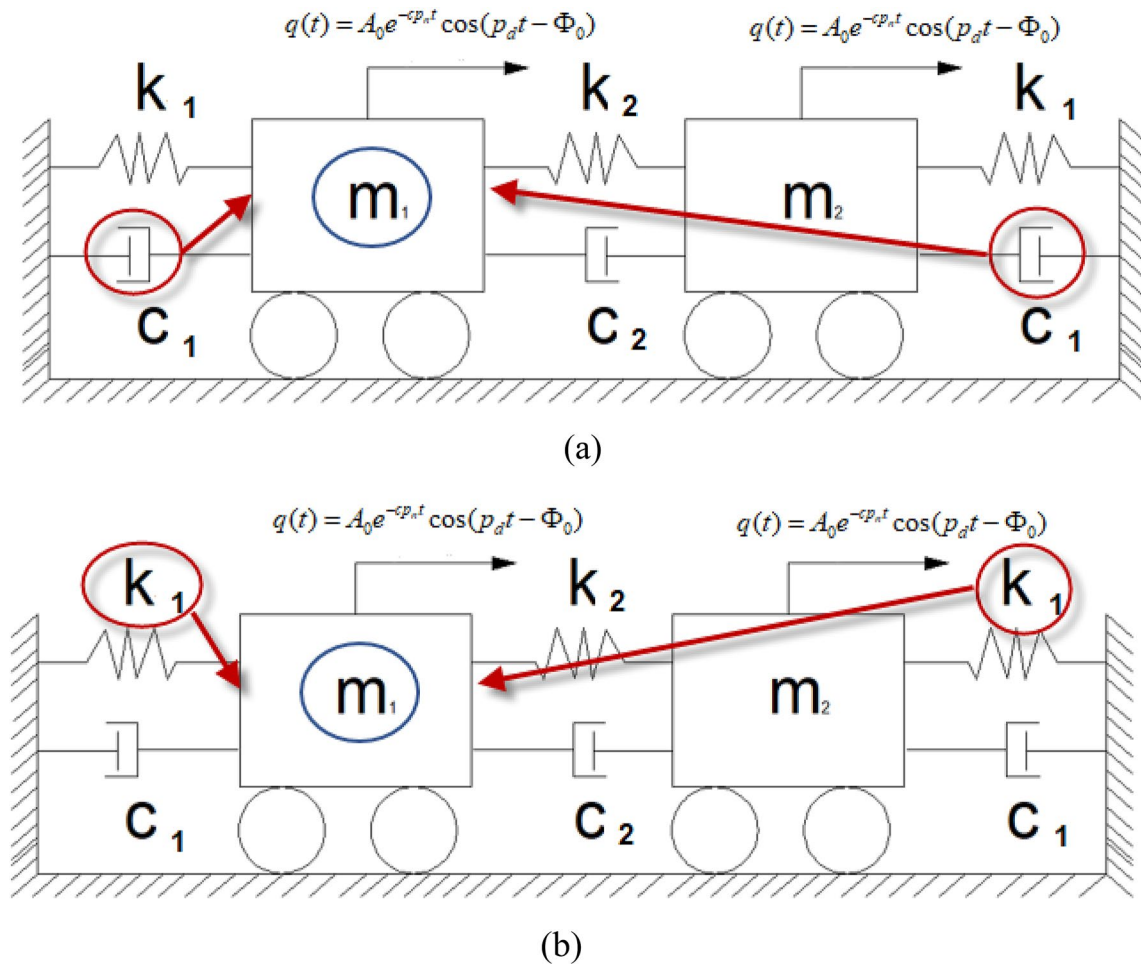


**Fig. 22** The two degrees of freedom discrete system to change both  $K_1$  and  $c_1$

In Fig. 17, FFT-deep learning produced more sensitive results than FT. Simultaneously, the variable damping coefficient matched the changes in the mechanical characteristics of structures in reality. It means that when the damping coefficient increases, the vibration amplitude decreases. In addition, the most decreasing component was the maximum amplitude value. However, the maximum frequency value tended to decrease only slightly. The value of the damping coefficient had little effect on the vibration frequency of structures.

#### Assessment of the Effects of Variable Mechanical Components on the Vibration Characteristics

Figure 18 shows the effects of the overall stiffness  $K$  and the damping  $c$  on the maximum vibration amplitude of the spectrum for FFT-deep learning and FT. The signal in FFT-deep learning analysis obtained more efficient results than in FT. The mechanical characteristics were affected by the

overall stiffness and damping of structures. However, in this circumstance, the spectral amplitude always appeared superior to the damping component.

Figure 18 shows that the mechanical characteristics of structures largely affected the maximum vibration amplitude as well as the natural vibration frequency. The damping component changed the vibration amplitude but did not have much effect on the vibration frequency of structures. This means that when the damping coefficient increases to a certain value, the maximum value of the spectral amplitude is no longer seen. Then, the maximum vibration amplitude decreases until the end (decreases by 100%). Therefore, if the vibration amplitude value is completely attenuated, a structure completely bears the load as in its static state. Then, the risk of suffering damage in the structure is relatively high. On the other hand, the stiffness component also affects the maximum vibration amplitude, although at a lower level.

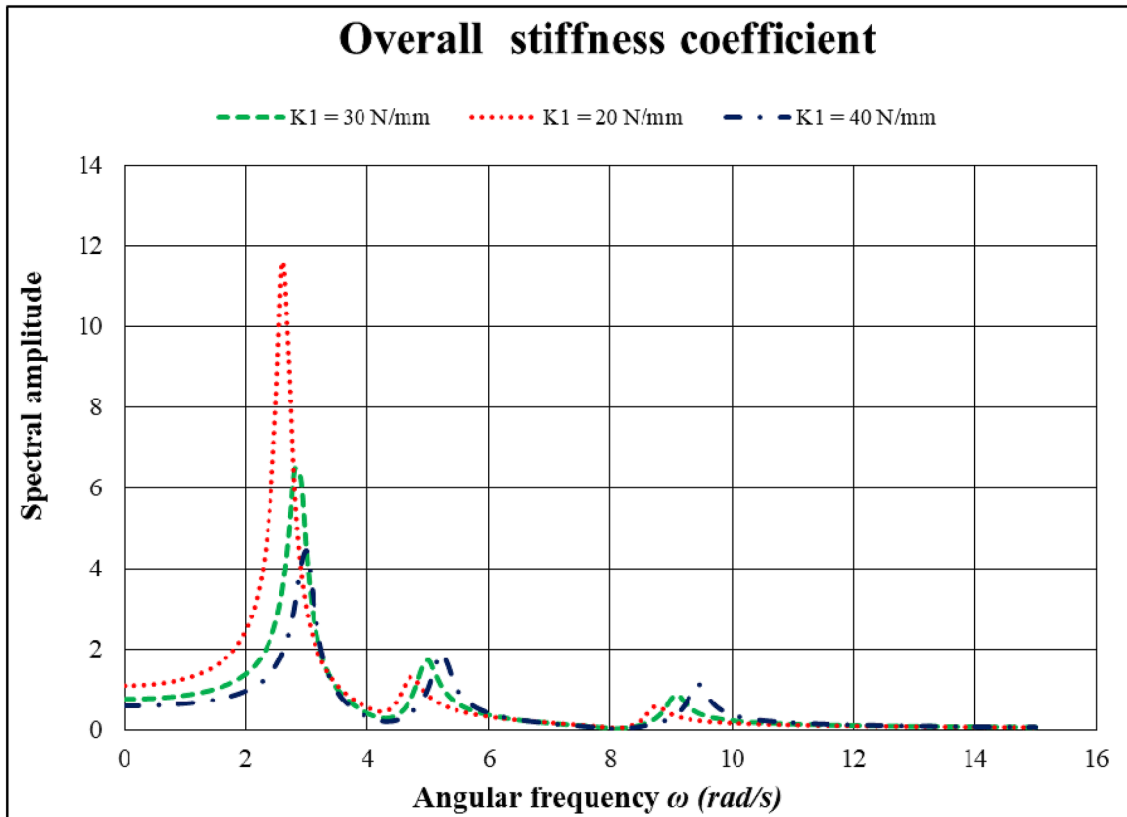


**Fig. 23** The effect of  $K_1$  on the mechanical characteristics of material with two degrees of freedom model

As shown in Fig. 19, the research observed the effects of damping coefficient and overall stiffness on the vibration frequency of structures (the resonant frequency). The changing process of these components shows that the one that significantly affected resonant frequency was overall stiffness value. At the same time, the damping coefficient had less effect on this parameter. Therefore, the structure had many changes in the amplitude of the spectrum due to the damping component. The reason was that this component suffered many factors such as working environment, weather, and load type. Besides this, the resonant frequency component tended to change very little as it was largely dependent on the overall stiffness. Therefore, it can be concluded that the damping component is the most varying mechanical characteristic in reality.

#### The Changes of Spectral Amplitude According to Each Resonant Area

Actually, the collected spectral amplitude of structures has not only one but also various resonant areas. These areas can be changed according to the collecting periods. The draft investigated how the resonant area changed at different frequencies and simultaneously commented on the

correspondence in comparison with reality. For two degrees of freedom, the spectral amplitude had two resonant areas, and three or four degrees of freedom followed the same rule. For a structure in reality, although it has been analyzed into  $n$  degrees of freedom, the largest number of resonant areas is only three. Changes in the mechanical characteristics of structures are shown by changes in each resonant area. The model for two degrees of freedom was investigated, as depicted in Fig. 3, and for three degrees of freedom as in Fig. 4.

Figures 20, 21 show that each resonant area of the vibration spectrum had different changes when the mechanical characteristics changed. However, the changing tendency of the attenuation process was a smaller number of resonant areas that are merged into a new area. In this process, the higher frequency area had a greater change than the lower frequency one. With even higher degrees of freedom, the changing reaction of vibration characteristics when the mechanical characteristics changed (using the two degrees of freedom discrete mechanical system with the change of both  $K_1$  and  $K_2$  and  $c_1$  and  $c_2$ ) is shown in Figs. 22 and 25.

The overall rules derived from changes in the mechanical characteristics of structures through multiple degrees of freedom share the following common points:

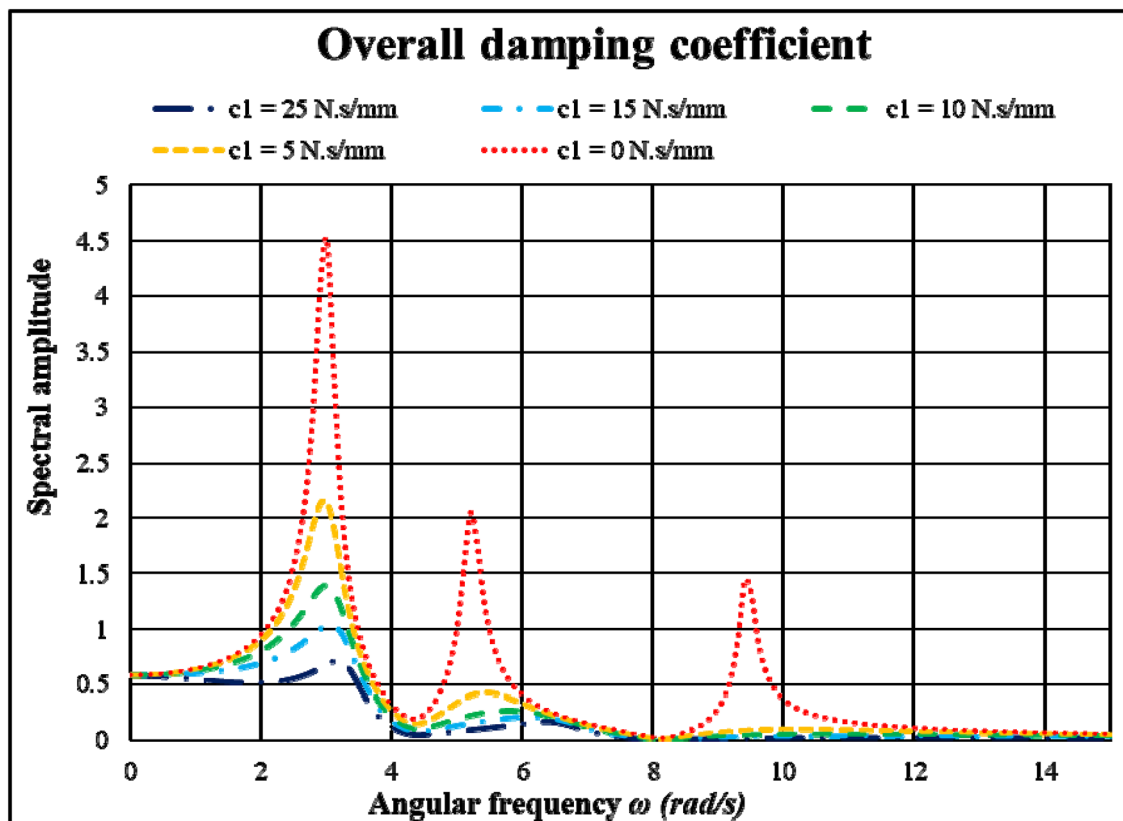


**Fig. 24** The effect of damping coefficient ( $c_1$ ) on the mechanical characteristics of materials with two degrees of freedom model

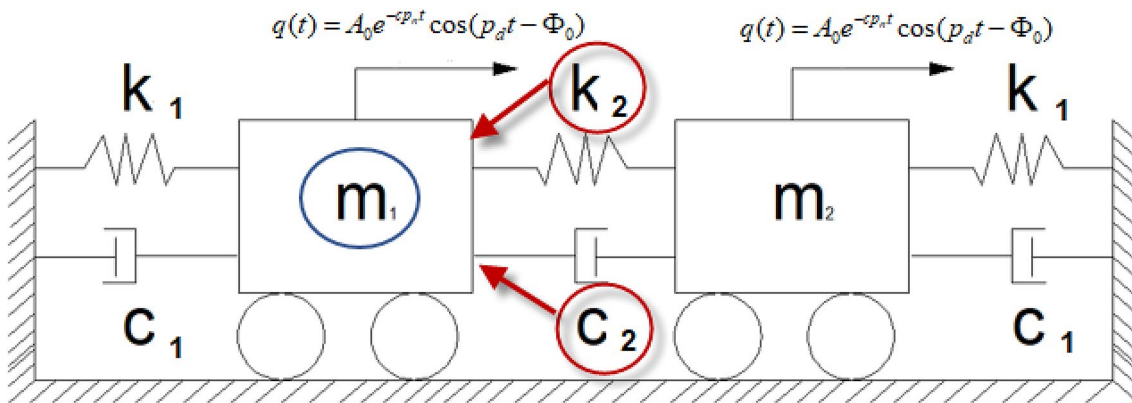


**Fig. 25** The two degrees of freedom discrete system to change both  $K_1$  and  $c_1$

- The resonant frequency area quickly altered and showed changes in the mechanical characteristics of structures. The highest frequency area had lower stability than other areas, which means that it could easily become unstable, lost or changed. Figures 23, 24, 25, 26, 27 show that variation in stiffness was the main reason for the change in frequency areas. Natural frequency values gradually decreased following changes

in the mechanical characteristics of structures. In addition, when the stiffness decreased, the phenomenon of gathering frequency values and increasing maximum amplitude of the spectrum is seen in the low frequency area. On the contrary, the resonant areas at higher frequency tended to sharply decrease and completely disappeared when the stiffness of structures sufficiently changed.



**Fig. 26** The effect of  $K_2$  on the mechanical characteristics of materials with two degrees of freedom model

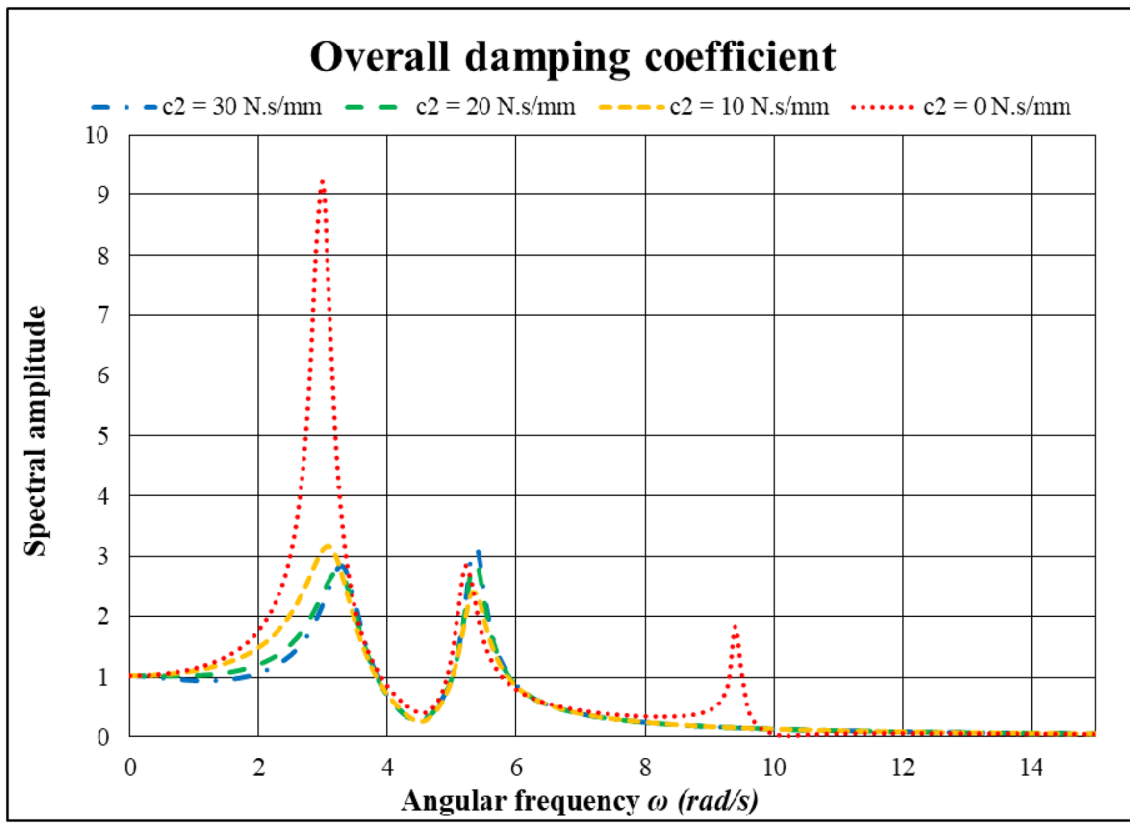
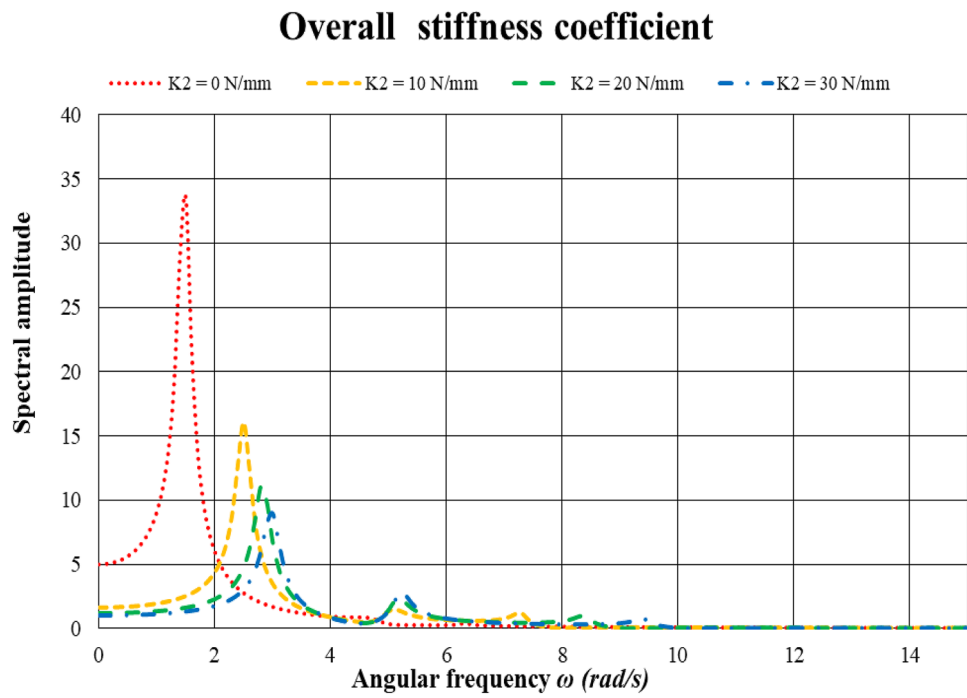


**Fig. 27** The effect of damping coefficient ( $c_2$ ) on the mechanical characteristics of materials with two degrees of freedom model

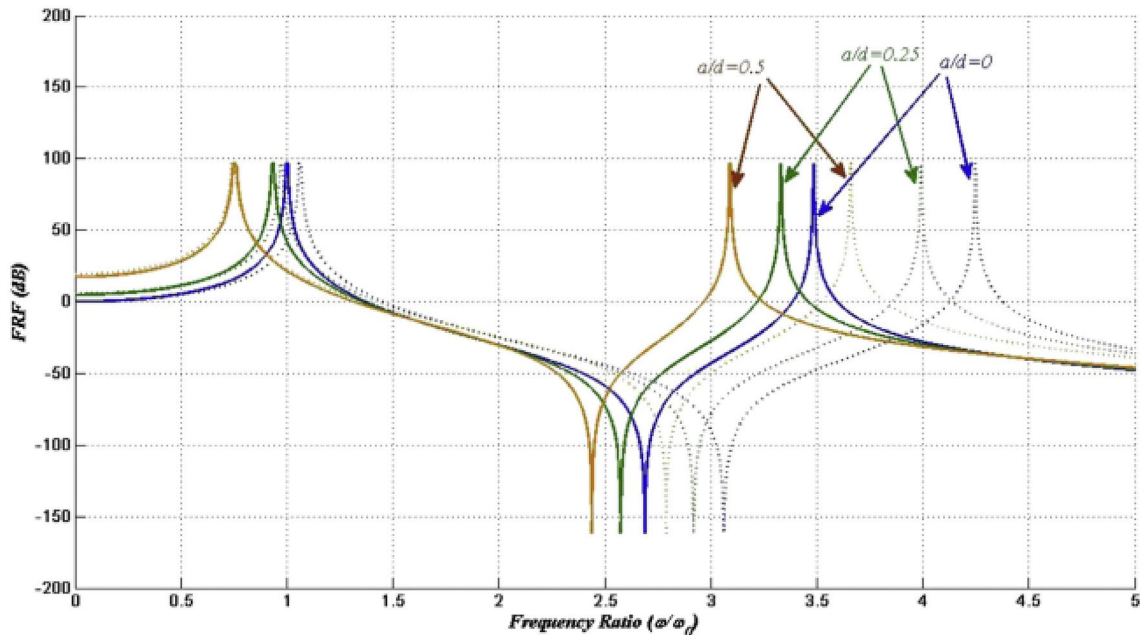


**Fig. 28** The effect of the overall stiffness ( $K$ ) on beam with a crack [35]

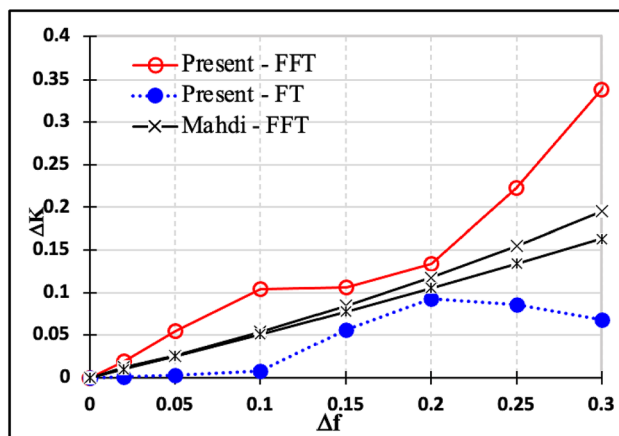


**Fig. 29** Comparison of the sensitivity between results given in [27] and in this study

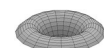
- The damping coefficient did not cause changes in the natural frequency value but affected the spectral amplitude of the resonant area. Almost all resonant areas tended to decrease in amplitude when the damping coefficient increased and disappeared entirely when the mechanical characteristics of structures completely changed.

The shifting phenomenon of resonance areas was observed by Mahdi Heydari et al. [35]. Under changes of the fault in the beam (shown by the crack), the area of resonance of frequencies tended to decrease from higher ranges

to lower ones, as shown in Fig. 28. The results are similarly shown in this study in Figs. 23, 24, 26, 27, which indicates that the nature of this shifting phenomenon has been successfully represented. The study reported in [35] only showed changes in the mechanical properties of structures through the overall stiffness ( $K$ ), which was characterized by changes in the crack, such as its degree of depth and its width in the beam. The research overlooked the influence of the material's mechanical properties in the presence of cracks in the beam. Using the reasoning from the study [35] only evaluates half of the issues arising from changes in structure. The highlight of this work lies in evaluating changes in a structure's mechanical properties based on both variations in the mechanical properties of the material as well as changes in the structure's stiffness, as shown in Fig. 29.

## Conclusion

The article evaluates changes in the mechanical characteristics of structures through the discrete model, Fast Fourier Transform (FFT) analysis and deep learning. The structured discrete model used in this research follows a completely new reasoning where a complex and continuous structure model is transformed into the simplest structure with one degree of freedom, two degrees of freedom or three degrees of freedom. This method allows simultaneous investigation of two components affecting the mechanical characteristics of structures during the vibration process, including the



overall stiffness ( $K$ ) and the damping coefficient ( $c$ ), while almost all the previous researches focus on only one of the two. The discrete model proposed in this research is totally different from the finite element method. The reason is this method only models the mechanical characteristics of a structure by finite degrees of freedom to minimize deviation and achieve the most realistic results. The research results show that the overall stiffness component of structures displaces the value and resonant area of the natural frequencies. However, the damping component only changes the amplitude of the spectrum without altering the value of the natural frequencies. To increase data analysis efficiency, the research uses FFT-deep learning to increase the sensitivity during the vibration process of structures. FFT-deep learning simplifies the calculations so the results are less affected by interference and deviation during the analytic process. The efficiency achieved from using FFT-deep learning increases by 25% in comparison with using traditional Fourier transform (FT) analysis. The research shows higher efficiency when using the structured discrete model and FFT-deep learning than when using only other models or analyses.

**Data Availability** All data generated or analyzed during this study are included in this work.

## References

- Bhardwaj G, Singh IV, Mishra BK (2015) Stochastic fatigue crack growth simulation of interfacial crack in bi-layered FGMs using XIGA. *Comput Methods Appl Mech Eng* 84:186–229
- Kunin B (2013) Stochastic model of brittle crack growth under cyclic load. *Int J Pure Appl Math* 84:163–174
- Yu H, Wu L, Guo L, Wu H, Du S (2010) An interaction integral method for 3D curved cracks in nonhomogeneous materials with complex. *Int J Solids Struct* 47:2178–2189
- Price RJ, Trevelyan J (2014) Boundary element simulation of fatigue crack growth in multi-site damage. *Eng Anal Boundary Elem* 43:67–75
- Bittencourt T, Wawrzynek P, Ingraffea A, Sousa J (1996) Quasi-automatic simulation of crack propagation for 2D LEFM problems. *Eng Fract Mech* 55:321–334
- Moës N, Dolbow J, Belytschko T (1999) A finite element method for crack growth without re-meshing. *Int J Numer Methods Eng* 46:131–150
- Sunde SL, Berto F, Haugen B (2018) Predicting fretting fatigue in engineering design. *Int J Fatigue* 117:314–326
- Vazquez J, Carpinteri A, Bohorquez L, Vantadori S (2019) Fretting fatigue investigation on Al 7075–T651 alloy: experimental, analytical and numerical analysis. *Tribol Int* 135:478–487
- Aeran A, Vantadori S, Carpinteri A, Siriwardane S, Scorza D (2019) Novel non-linear relationship to evaluate the critical plane orientation. *Int J Fatigue* 124:537–543
- Bhatti NA, Wahab MA (2017) Finite element analysis of fretting fatigue under out of phase loading conditions. *Tribol Int* 109:552–562
- Bhatti NA, Wahab MA (2018) Fretting fatigue crack nucleation: a review. *Tribol Int* 121:121–138
- Hojjati-Talemi R, Wahab MA, De Pauw J, De Baets P (2014) Prediction of fretting fatigue crack initiation and propagation lifetime for cylindrical contact configuration. *Tribol Int* 76:73–91
- Nguyen TQ, Nguyen HB (2021) Detecting and evaluating defects in beams by correlation coefficients. *Shock Vib* 2021:6536249
- Nguyen TQ, Tran LQ, Nguyen-Xuan H, Ngo NK (2021) A statistical approach for evaluating crack defects in structures under dynamic responses. *Nondestruct. Test Eval* 36(2):113–144
- Ngo NK, Nguyen TQ, Vu TV, Nguyen-Xuan H (2020) An fast Fourier transform-based correlation coefficient approach for structural damage diagnosis. *Struct Health Monit*. <https://doi.org/10.1177/1475921720949561>
- Nguyen TQ, Nguyen TTD, Nguyen-Xuan H, Ngo NK (2019) A correlation coefficient approach for evaluation of stiffness degradation of beams under moving load. *Comput Mater Continua* 61(1):27–53
- Kolekar S, Venkatesh K, Oh JS et al (2019) Vibration controllability of sandwich structures with smart materials of electrorheological fluids and magnetorheological materials: a review. *J Vib Eng Technol* 7:359–377
- Khiem NT, Lien TV (2001) A simplified method for natural frequency analysis of a multiple cracked beam. *J Sound Vib* 245(4):737–751
- Ebrahimi A, Heydari M, Behzad M (2018) Optimal vibration control of rotors with an open edge crack using an electromagnetic actuator. *J Vib Control* 14(1):37–59
- Zhang QW (2007) Statistical damage identification for bridges using ambient vibration data. *Comput Struct* 85(7–8):476–485
- Li ZX, Chan HT, Zheng TR (2003) Statistical analysis of online strain response and its application in fatigue assessment of a long-span steel bridge. *Eng Struct* 25(14):1731–1741
- Ayaho M, Kei K, Hideaki N (2000) Bridge management system and maintenance optimization for existing bridges. *Comput-Aided Civil Infrastruct Eng* 15(3):45–55
- Furuta H, He J, Watanabe E (1996) A fuzzy expert system for damage assessment using genetic algorithms and neural networks. *Microcomput Civil Eng* 11(1):37–45
- Mares C, Surace C (1996) Application of genetic algorithms to identify damage in elastic structures. *J Sound Vib* 195(5):195–215
- Sharma V, Raghuwanshi NK, Jain AK (2021) Sensitive sub-band selection criteria for empirical wavelet transform to detect bearing fault based on vibration signals. *J Vib Eng Technol*. <https://doi.org/10.1007/s42417-021-00316-8>
- Yun CB, Bahng EY (2000) Structural identification using neural networks. *Comput Struct* 77(1):41–52
- Chang CC, Chang TY, Xu YG (2000) Structural damage detection using an iterative neural network. *J Intell Mater Syst Struct* 11(1):32–42
- Huang CS, Hung SL, Wen CM, Tu TT (2003) A neural network approach for structural identification and diagnoses of a building from seismic response data. *Earthquake Eng Struct Dynam* 32(2):187–206
- Zhu XQ, Law SS (2006) Wavelet-based crack identification of bridge beam from operational deflection time history. *Int J Solids Struct* 43(7–8):2299–2317
- Douka E, Loutridis S, Trochidis A (2003) Crack identification in beams using wavelet analysis. *Int J Solids Struct* 40(13–14):3557–3569
- Anantha Ramu S, Johnson VT (1995) Damage assessment of composite structures: a fuzzy logic integrated neural network approach. *Comput Struct* 57(3):491–502
- Ambhore N, Kamble D, Chinchanikar S (2020) Evaluation of cutting tool vibration and surface roughness in hard turning of

- AISI 52100 steel: an experimental and ANN approach. *J Vib Eng Technol* 8:455–462
33. Malla C, Panigrahi I (2019) Review of condition monitoring of rolling element bearing using vibration analysis and other techniques. *J Vib Eng Technol* 7:407–414
34. Nguyen TQ, Vuong LC, Le CM, Ngo NK, Nguyen-Xuan H (2020) A data-driven approach based on wavelet analysis and deep learning for identification of multiple-cracked beam structures under moving load. *Meas J Int Meas Confed* 162:107862
35. Heydari M, Ebrahimi A, Behzad M (2014) Forced vibration analysis of a Timoshenko cracked beam using a continuous model for the crack. *Eng Sci Technol Int J* 17:194–204
36. Nguyen SD, Ngo KN, Tran QT, Choi SB (2013) A new method for beam-damage-diagnosis using adaptive fuzzy neural structure and wavelet analysis. *Mech Syst Signal Process* 39(1–2):181–194

**Publisher's Note** Springer Nature remains neutral with regard to jurisdictional claims in published maps and institutional affiliations.